Egypt. J. Chem. **Vol. 68,** No. 10 pp. 511 - 530 (2025)

Egyptian Journal of Chemistry

http://ejchem.journals.ekb.eg/

Utilizing of Heavy Metal Ions Adsorption by New Urea-Based-Polyvinyl chloride Solid Support: Equilibrium and Thermodynamic Characteristics

Abd El-Hakeim T. Kandil[a], Bahig M. Atia[b]*, Mohamed Y.M. Hussein[a], Farida M.S.E. El-Dars[a], Hani E. Sharafeldin[c], Mohamed F. Cheira[b]

[a] *Chemistry Department, Faculty of Science, Helwan University, 11795 Cairo, Egypt.*
[b] *Nuclear Materials Authority, El Maadi P.O. Box 530, Cairo, Egypt.*
[c] *Al-Azhar University, Faculty of Engineering, Minning and Pet. Dept., Nasr City, 11371, Cairo, Egypt.*

Abstract

A new urea-modified polyvinyl chloride composite (PVC-urea) has been strategically synthesized and rigorously characterized as a prospective sorbent for the efficient extraction of uranyl ions from solutions. Comprehensive spectroscopic and analytical techniques, including FT-IR, ^{1}H-NMR, SEM-EDX, ^{13}C-NMR, TGA, and GC/MS, have been employed to confirm the successful fabrication and structural integrity of the PVC-urea composite. The adsorption performance of the synthesized material has been meticulously optimized by systematically investigating the influence of key operational strictures, likes, pH, initial uranyl ion concentration, contacting time, adsorbent dosage, and competing ions, temperature, and the efficacy of various eluting agents. Under optimized conditions (25 °C, pH 4.5, 10 minute agitation, and an initial uranyl ion concentration of 0.63×10^{-3} mol/L), the PVC-urea composite demonstrated a maximum uranyl ion uptake ability of 25 mg/g. Adsorption isotherm analysis revealed a superior fit to the Langmuir modelling reviewed to the Freundlich modelling, with a theoretical extreme adsorption capacity of 24.1 mg/g, closely aligning with the experimentally determined value. Kinetic judges indicated that the adsorption manner is well-described by a mixed pseudo-first order and pseudo-second order model, yielding theoretical retention capacities of 25.35 mg/g and 25.31 mg/g, respectively. Thermodynamic analysis suggests that the adsorption process is exothermic (ΔH = -10.62 kJ/mol) and non-spontaneous, as evidenced by positive Gibbs free energy values ranging from 3.43 to 6.1 kJ/mol at 298 to 353 K, with favorable adsorption observed at lower temperatures (ΔS = -0.0472 kJ/mol). Furthermore, quantitative recovery of the adsorbed uranyl ions was achieved with high efficiency (97%) using 0.5 M H_2SO_4 as an eluting agent, underscoring the economic viability of the process. The PVC-urea composite exhibited notable selectivity towards uranyl ions in the attendance of a range of common co-ions, demonstrating a robust tolerance limit and highlighting its potential for selective uranyl ion extraction in complex environmental matrices.

Keywords: Urea-based-polyvinyl chloride; Adsorption; Elution; Uranyl ions; Kinetics; Thermodynamics

1. Introduction

Uranium, a strategically significant heavy metal, constitutes a cornerstone of global energy architecture by virtue of its indispensable role in nuclear fuel production [1]. Dispersed within the Earth's crust at a mean of 4 mg/L, uranium is judiciously concentrated through natural geological processes, yielding economically exploitable ore bodies within varied lithological settings. Within these deposits, uranium predominantly exists as primary minerals, notably Uraninite, Pitchblende, and Coffinite, wherein the element is characterized by its tetravalent oxidation state. Conversely, secondary uranium minerals, exemplified by Autunite, Uranophane, and Kasolite, manifest uranium in its hexavalent form, arising from weathering and alteration processes. The extraction of uranium from these ores is commonly accomplished via leaching, employing either acidic or alkaline solutions to mobilize the target element. Subsequent to leaching, the uranium is selectively recovered from the resultant pregnant leach solution through well-established systems, includings solvent extraction or ion exchange, ensuring efficient separation and purification of the uranium. This refined material serves as a critical feedstock for downstream applications, primarily within the nuclear fuel cycle, but also extending to other specialized technological domains requiring its unique properties [2, 3].

The imperative for efficient and highly selective uranium recovery and separation has catalyzed extensive research into advanced ion exchange resin materials, driving innovation across the field. Significant advancements have been achieved through the exploration of Alizarin red-S modified anion exchange resins, which strategically exploit the complexation characteristics of Alizarin red-S to achieve enhanced uranium binding capabilities [4]. Concurrently, substantial research efforts have focused on the development and comprehensive characterization of co-polymeric resins formulated from acryl amide-methyl-propane-sulphonic acid and acrylic acid [5], linked with methylene-bis-acrylamide. These materials exhibit considerable promise for uranium extraction, attributable to the synergistic functionalities afforded by the strategic combination of the two monomers, resulting in improved binding affinity and selectivity. Complementary investigations into cross-linked acrylic acid acrylonitrile copolymer resins have further illuminated their efficacy in uranium sequestration,

---

*Corresponding author e-mail: dr_bahig.atia@yahoo.com.; (Bahig Mohamed Atia).

Received date 07 February2025; revised date 06 March2025; accepted date 09 March2025
DOI: 10.21608/ejchem.2025.358926.11279

underscoring the critical role of precise polymer composition and controlled crosslinking density in optimizing overall resin performance and maximizing uranium uptake [6].

The feasibility of using exchanging resins for the selective capture of uranium(VI) from various matrices is highlighted by a thorough evaluation of relevant literature. Specifically, strong base anion exchanging resins likes Ambersep 920U Cl, have demonstrated efficacy in extracting anionic uranyl sulfate complexes, namely $[UO_2(SO_4)_2]^{2-}$ and $[UO_2(SO_4)_2]^{4-}$, from complex saline solutions, as evidenced by studies conducted on Abu Zeneima ore samples originating from South Western Sinai, Egypt [7]. Conversely, amino phosphonic acid chelating resins, such as Amberlite IRC-747, exhibit preferential affinity for the uranyl cation (UO_2^{2+}), enabling the recapture of U(VI) and U(IV) from challenging industrial streams like Abu Zaabal wet phosphoric acid [8].

The purposeful chemical and physical functionalization of sturdy solid supports with chelating active sites affords a promising route for the selective removal and recovering of precious metals from complicated matrices. In this vein, a pyridylazoresorcinol/Amberlite XAD-16 resin has demonstrated notable efficacy in the recovery of U(VI), exhibiting a significant sorption capacity of 115.5 mg/g [9]. Complementary research efforts have leveraged the impregnation method to facilitate uranium recovery, highlighting the versatility of Amberlite XAD-16 as a solid support. Notably, dibutyl-benzoyl thiourea impregnation has been successfully employed for this purpose [10], alongside quinizarin impregnation, further expanding the repertoire of functional ligands for uranium extraction [11]. Beyond these examples, investigations have explored the potential of alternative chelating agents, including dihexylcarbamoylmethyl phosphonic acid [12], 3dihydroxybenzoylmethyl phosphonic acid [13], and (bis-dihydroxybenzoyl)-p-phenylenediamine [14], demonstrating a concerted effort to optimize and diversify solid-phase extraction methodologies for uranium recovery, thereby contributing to advancements in resource management and sustainable extraction technologies.

Several investigations have explored the efficacy of diverse resin materials in selectively recovering uranium(VI) from various aqueous matrices. A comparative analysis of commercially available chelating resins (Lewatit OC-1060, Diphonix, Purolite S940, and Diaion-CRP200) has been conducted to assess their performance in extracting U(VI) from phosphoric acid solutions [15]. Furthermore, researchers have synthesized novel chitosan-based resins, specifically chitosan amine (CR-amine) and chitosan azole resin (CR-azole), through the cross-linking of chitosan polymer with glutaraldehyde, followed by subsequent reactions with ethylene diamine and (amino-triazole-thiol), respectively. These resins exhibited notable uranium uptake capacities of 309.4 and 428.4 mg/g [16]. In another approach, a Merrifield chloromethylated resin was attached with octyl(phenyl)-diisobutylcarbamoyl-methylene phosphine oxide, resulting in a material suitable for uranium recovery from nuclear waste streams, demonstrating a sorption capacity of 228.48 mg/g [17]. Similarly, the grafting of N, N-dihexyl succinic acid onto Merrifield chloromethylated resin has been successfully employed for uranium extraction from highly acidic environments, such as 4M HNO_3, achieving a supreme sorption capability of 157.08 mg/g [18]. Beyond modified Merrifield resins, Amberlite XAD-4 modified with oxine was also studied; it was effectively utilized for the U(VI) extraction and preconcentration from solutions within a pH range of 4-5.5 [19]. The chelating potential of a robust tris-biphosphonic ligand towards uranyl ions has also been investigated [20]. For solid-phase extraction applications, a Merrifield chloromethylated resin/calix[4]arene-vanillin-semicarbazone was synthesized, demonstrating a considerable sorption capacity of 48734 mg/g for U(VI) preconcentration at pH 6-7 [21]. Furthermore, Duolite XAD-761/phenyl-fluorone chelate has been developed for the selective separation of U(VI) [22]. Finally, tetramethyl malonamide/Merrifield chloromethylated resin was synthesized as another method for U(VI) elimination from acidic forms, exhibiting a noteworthy sorption capacity of 125 mg/g [23].

The efficacy of chelating resins for the choosy deletion of U(VI) has garnered considerable attention, prompting investigations into novel ligand functionalities and support matrices. In this context, the complexation behavior of a resin incorporating a bicine ligand was rigorously examined, revealing a maximum uranium uptake capacity of 90.44 mg/g [24]. Further advancements in resin design include the successful of (trihydroxybenzyl) ethylenediamine/Amberlite XAD-16, yielding a material capable of extracting U(VI) with a significantly enhanced uptake capability of 340.34 mg/g [25]. Demonstrating substantial progress in this domain, the submission of a polymer-supported calix[6]arenehydroxamic acid for U(VI) sequestration at pH 4 resulted in an impressive uptake capacity of 1061.48 mg/g [26], underscoring the potential of tailored macrocyclic ligands for achieving highly efficient uranium recovery from complex aqueous systems.

Advanced methodologies for uranium extraction and preconcentration have witnessed significant progress through the application of functionalized polymeric resins. Notably, selective uranium separation has been achieved utilizing a chelating resin synthesized by incorporating tert-butyl calix[8]arene and polymeric Amberlite XAD-4 matrix, demonstrating a noteworthy uptake capacity of 173.74 mg/g [27]. Furthermore, the efficacy of dimethyl aminophosphonomethyl-phosphonic acid/Merrifield chloromethylated resin has been displayed for U(VI) preconcentration from monazite sand, exhibiting a superior uptake capacity of 2.02 mmol/g [28]. In alternative approaches, silica-supported vinylpyrrolidone has been successfully synthesized and employed for the choosy withdrawal of U(VI) from nitric acid media, highlighting the versatility of modified silica substrates in uranium recovery [29]. Complementing these advancements, anionic exchange resins, specifically Dowex 1-X8 and Purolite A-520E, have been identified as highly effective adsorbents for U(VI), displaying a substantial accumulative uptake capacity of approximately 49.8 mg/g at pH 5, underscoring their potential for efficient uranium capture under optimized conditions [30].

Amides represent a cornerstone functional group within organic chemistry, holding profound significance across a diverse spectrum of disciplines, including pharmaceutical development, the characterization of naturally occurring molecules, the engineering of advanced polymeric materials, and the formulation of effective agrochemicals [31]. Consequently, the synthesis of carboxamides constitutes a pivotal endeavor in organic, medicinal, and coordination chemistry, frequently achieved through amidation by reaction meticulously engineered utilizing carboxylic and amine groups. While conceptually straightforward, amidation is fundamentally an equilibrium-driven process, initially involving an acid-base interaction that yields a stable salt intermediate. Critically, the formation of the desired amide bond must overcome an inherently unfavorable thermodynamic equilibrium, which typically favors hydrolysis of the amide linkage over its de novo synthesis [32, 33].

This research presents the development and implementation of a new polyvinyl chloride-urea composite (PVC-urea) meticulously synthesized for the selective deletion of U(VI) from solutions. The newly synthesized PVC-urea was comprehensively characterized utilizing a suite of advanced instrumental techniques, confirming its successful functionalization and structural integrity. Rigorous optimization studies were supervised to regulate the optimal parameters governing both the adsorption and subsequent elution processes, ensuring maximal efficiency and efficacy in uranium extraction. Furthermore, a thorough physico-chemical investigation was undertaken to elucidate the kinetic mechanisms, equilibrium isotherms, and thermodynamic principles underpinning the uranium adsorption process, providing a comprehensive understanding of the interaction between the PVC-urea composite and uranyl ions in solution. This holistic approach offers valuable insights into the potential application of PVC-urea as an effective and sustainable sorbent material for uranium recovery and environmental remedy.

2. Experimental

2.1. Instrumentation

Quantitative analyses were conducted utilizing a suite of sophisticated instrumentation to ensure the rigor and reliability of the experimental results. Precise mass measurements of all samples were obtained using a Sartorius TE analytical weigh, characterized by a 10^{-5} g sensitivity, providing a high degree of accuracy in gravimetric assessments. Hydrogen ion concentrations were determined with a Digimed digital pH meter (Japan), exhibiting a measurement uncertainty of ±0.1 pH units. Equilibrium experiments were performed by agitating a precisely weighed quantity of synthesized chelating composites with a defined volume of uranyl ion-containing solution using a Vibromatic-384 shaker to facilitate efficient interaction and mass transfer. The concentration of uranyl ions was quantitatively determined via spectrophotometry, employing a Meterch Inc. SP-8001 single-beam spectrometer. Inductively Coupled Plasma Optical Emission Spectrometry (ICP-OES, USA) was implemented for both the speciation of uranyl ions and the determination of tolerance limits for co-existing ionic species. Structural characterization was achieved through Fourier Transform Infrared (FT-IR) spectroscopy, with fields developed using an FT-IR 4100 Gasco-Japan spectrometer, employing the KBr disk method. Nuclear Magnetic Resonance (NMR) spectroscopy, encompassing both ^{1}H and ^{13}C nuclei, was performed on a mercury 400 Bruker spectrometer. These spectroscopic analyses were pretended at an exact temperature (293 K) on diluted solutions prepared in DMSO solvent. Chemical shifts (δ) are testified in ppm, and coupling constants (J) are informed in Hertz (Hz). Further chemical identification and structural elucidation were achieved using gas chromatography-mas spectrometry (GC/MS) considerations, which were implemented on a Shimadzu Plus spectrophotometer. Elemental composition was determined using a Perkin-Elmer Elemental analyzer (Rotkrewz, Switzerland). The thermal stability of the integrated substances was assessed via thermo-gravimetric analysis (TGA), conducted under a nitrogen atmosphere operating a Shimadzu TGA thermal analyzer. Finally, the elemental composition of the produced compounds was finalized via Energy Dispersive X-ray spectroscopy (EDX) utilizing a JSM apparatus (Japan), providing spatially resolved elemental information.

2.2. Reagents and chemicals

The reliability and precision of the experimental results were guaranteed by the diligent use of analytical reagents of the highest purity grade throughout this inquiry. In particular, the German pharmaceutical company Merck supplied the uranyl acetate dihydrate and Arsenazo III, demonstrating their commitment to rigorous quality control measures. Polish company POCH supplied the analytical grade polyvinyl chloride (PVC), HCl, H_2SO_4, and HNO_3. Sodium hydroxide, ammonium vanadate, sodium nitrite, and ferrous sulfate heptahydrate were purchased from the illustrious Spanish supplier Scharlau Chemie. The experimental procedures also relied on solvents acquired from Scharlau Chemie, Spain, such as urea, methanol, ethyl acetate, and N,N-dimethylformamide (DMF). Every solvent was first subjected to stringent purification procedures using time-tested laboratory methods. This process ended with fresh distillation to ensure the solvent was as pure as possible and free of any impurities. To further exclude the possibility of adventitious moisture affecting reaction kinetics or yields, all synthetic processes were carried out in flame-dried glassware.

To create a carefully made U(VI) stock solution with a concentration of 4.2×10^{-3} M, a specific amount of uranyl acetate was dissolved in 1000 mL of extracted water and then acidulated with 3 mL of concentrated sulfuric acid to prevent hydrolysis. In addition, 1000 mg/L standard stock solutions of various ions that could interfere with U(VI) elimination by the PVC-urea combination were trained by dissolving the corresponding masses of salts in 1000 mL of distilled water. These solutions were designed to cover all bases. The dedication to preserving the authenticity and reliability of the experimental results is demonstrated by this methodical strategy for reagent manufacture and purification.

2.3. Preparation of leach solution

Percolation leaching was strategically implemented to extract uranium from the G.Gattar ore sample, which presented an initial uranium concentration of 1.34 g/L. Rigorous optimization of key leaching parameters which included a leaching duration of 2 hours, a sulfuric acid of 75 g/L, a size of -100 mesh, ambient temperature, and a 1:2 solid/liquid ratio were squarely steered to maximize extraction efficiency. The resultant leach liquor yielded a uranium concentration of approximately 0.45 g/L. Subsequently, a precisely measured quantity of this G.Gattar leaching liquid (3 L) was subjected to batch-static treatment involving controlled agitation with a pre-determined mass of PVC-urea composite material. Comprehensive chemical characterization of both the G.Gattar ore and its associated leach liquor was performed utilizing colorimetry for the quantification of major oxides and ICP-OES for the precise purpose of trace element concentrations. The complete analytical data set is presented in tabular form for detailed analysis and interpretation, as detailed in Tables 1, 2, and 3.

Table 1. The major oxides of G.Gattar ore material.

Oxide	SiO_2	Al_2O_3	Fe_2O_3	FeO	CaO	MgO	P_2O_5	Na_2O	K_2O	MnO	TiO_2
Wt, %	68.6	8.16	2.59	0.14	6.73	0.6	0.02	2.35	3.38	0.07	0.15

Table 2. Trace elements of G.Gattar ore sample.

Element	Ba	Mo	Ni	Zr	Pb	Rb	Sr	Cu	Y	Zn	Nb	U
Conc., g/L	0.342	0.228	0.034	0.170	0.036	0.404	0.038	0.065	0.064	0.2	0.225	1.34

Table 3. The chemical alignment of G.Gattar leaching liquid.

Ions	Si^{4+}	Al^{3+}	Fe^{3+}	Mo^{6+}	V^{5+}	SO_4^{2-}	P^{5+}	Na^+	K^+	Zr^{4+}	Ti^{4+}	UO_2^{2+}
Conc., g/L	2.33	3.11	1.31	0.06	0.11	1.5	0.07	2.11	2.87	0.05	0.03	0.45

2.4. Static adsorption steps

The efficacy of a novel PVC-urea composite for the deletion of U(VI) from artificial solutions via adsorption was rigorously investigated utilizing a batch-static technique, with a focus on optimizing key operational parameters. This study systematically examined the influence of pH, composite dosage, contacting time, initial U(VI) ion, temperature, and the incidence of diverse ionic species on the adsorption process. In an illustrative test, 25 mL aliquots of solution, characterized by an initial concentration of 150 mg/L were subjected to mechanical agitation at a rate of 250 rpm in the presence of 0.05 g of the PVC-urea composite for defined durations across a range of controlled temperatures. The Uranium(VI) uptake capacity of the composite, denoted as q_e and expressed in mg/g as shown in Eq. 1, was subsequently determined through the product of a specific mathematical modelling, enabling a quantitative judgment of the adsorbent's performance under varying conditions.

$$q_e = (C_o - C_e) \times [\frac{v}{m}] \ldots\ldots\ldots\ldots\ldots..(1)$$

V is the volume of the liquid solution (L) comprising U(VI), m is the dry material weight (g), and C_o and C_e are the initial and balanced U(VI) contents (mg/L). At the same time, the distribution index (K_d) is determined by plugging the aqueous phase's volume (v) into Eq. 2:

$$K_d = \frac{C_o - C_e}{C_o} \times [\frac{v}{m}] \ldots\ldots\ldots\ldots\ldots.(2)$$

2.5. Static elution steps

To optimize the uranium(VI) recovery process from the PVC-urea chelating composite, a systematic investigation was conducted evaluating the efficacy of various eluting agents for the quantitative extraction of U(VI). This involved a series of rigorously controlled batch experiments where 0.05 g aliquots of the U(VI)-loaded resin were subjected to contact with 10 mL of carefully prepared eluting agent solutions, spanning a range of concentrations. Each elution procedure was meticulously executed under controlled laboratory conditions, maintaining a constant contact time of 30 minutes at ambient temperature, thus ensuring reproducibility and enabling a robust comparative analysis of eluting agent performance based on the extent of U(VI) re-extraction achieved. This approach allowed for a discerning assessment of the relative effectiveness of each eluting agent in disrupting the U(VI)-chelating composite interaction, paving the way for the selection of the most efficient and economically viable eluent for downstream uranium recovery applications.

2.6. Steps for U(VI) analysis

The quantification of U(VI) across diverse aqueous matrices was rigorously performed employing a Meterch SP-8001 single-beam spectrophotometer. Specifically, the spectrophotometric analysis leveraged the high sensitivity and selectivity of the Arsenazo III indicator [34], with absorbance measurements conducted at a meticulously controlled wavelength of 650 nm. Calibration curves were generated using certified U(VI) standard solutions to ensure accurate and precise analyte determination. To validate the integrity of the spectrophotometric findings, an independent analytical approach based on oxidometric titration following the well-established Davies and Gray method was implemented. This method involved titrating U(VI) against ammonium meta-vanadate, utilizing N-phenyl anthranilic acid as a visual indicator for endpoint determination [35, 36]. This dual-method approach, incorporating both spectrophotometry and titrimetry, provided a robust and defensible analytical strategy for the comprehensive assessment of U(VI) concentrations in the investigated aqueous phases.

3. Results and Discussion

3.1. Synthesis of urea-based-polyvinyl chloride composite (PVC-urea)

The urea-modified polyvinyl chloride (PVC-urea) composite material was meticulously synthesized through a single-stage reflux reaction. Specifically, a homogenous mixture comprising 0.16 moles of urea (approximately 9.6 g), 0.16 moles of PVC (approximately 10 g), and 0.16 moles of sodium hydroxide (6.4 g) was subjected to controlled heating at 100 °C for a duration of 5 hours within a reflux condenser. Dimethylformamide (DMF), carefully selected for its solvent properties, served as the reaction medium with a volume of 50 mL. The reaction's progression was rigorously monitored via ascending paper chromatography (PC), employing chromatographic sheets and an optimized eluent system consisting of ethanol and ethyl acetate. Subsequent visualization of the separated components was achieved through ultraviolet (UV) irradiation. Following the completion of the reaction, the PVC-urea composite was isolated by controlled cooling and subjected to iterative washing with absolute ethanol to ensure the complete removal of residual DMF and any generated by-products. The refined precipitate was then dried up at 111 °C for 3 hours, yielding the final PVC-urea outcome characterized by a density of around 1.17 g/cm^3. The synthetic pathway for the functionalization of polyvinyl chloride with urea, leading to the PVC-urea composite, lengthways with the planned reaction mechanism, are elucidated in Schemes 1 and 2, providing an inclusive considerate of the chemical transformation.

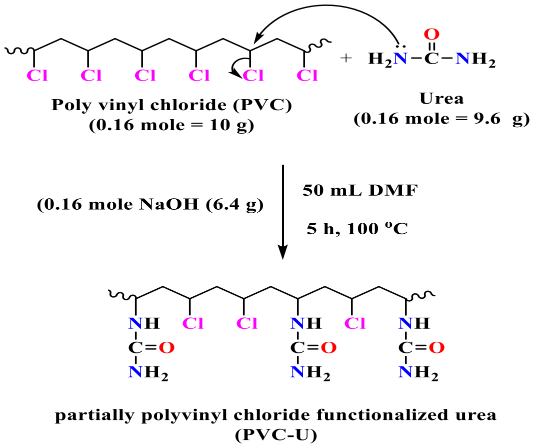

Scheme 1. Synthesis of urea-based-polyvinyl chloride composite.

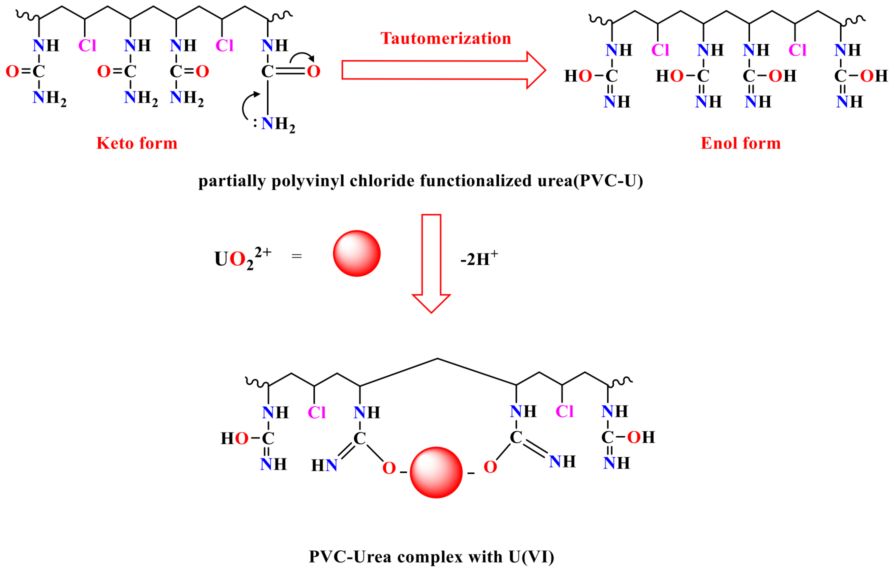

Scheme 2. An anticipated mechanism for U(VI) and PVC-urea.

3.2. Specification of Polyvinyl chloride functionalized urea

The yield was retrieved to be ≈ 12 g; **m.p** ≈ 265-270 °C; **FT-IR(KBr) v/cm^{-1}**= 3417 (-OH), 2846, 2908, 2962 (-CH aliphatic), 1249 (-C-N), 3209, 3255 (-NH), 493, 424 (-C-Cl), 1743 (-C=O), 1095 (-C-O) and 840, 964, 609 (-U-O). **^{1}H-NMR (400.16 MHz, DMSO-*d*$_6$, 25 °C, TMS)δ, ppm:** 1.74 (t, 2H, $(-CH_2)_n$, J=7 Hz), 4.1 (m, 1H, $(-CHCl)_n$, J=7.01 Hz), 3.87 (m, 1H, $(-CH\text{-}NH-)_n$, J=7 Hz), 6.07 (d, 1H, -NH, J=8.11 Hz), 5.67 (s, 2H, $-NH_2$). **^{13}C-NMR (100.04 MHz, DMSO-*d*$_6$, 25 °C, TMS)δ, ppm:** 55 (s, -CH-Cl, J= 3.3 Hz), 42.65 (s, $(-CH_2)_n$, J= 3.3 Hz), 44.15 (s, $-CH\text{-}NH\text{-}CO\text{-}NH_2$, J= 1.9 Hz), 159.03 (s, -C=O, J=

3.2 Hz). **GC-MS (EI, 30 eV), m/z (% rel): [m/z]$^+$**:106, 78, 125, 91, 105, 128, 142, 156, 178, 36, 17, 44, 108, 158, 42, 27, 54, 112, 147, 60, 62, 43. **Anal. Calc. for $[C_3H_6N_2O]_{n=1}$**building unit(106 g/mol): **C**, 33.96; **H**, 5.66; **N**, 45.28; **O**, 15.1. **Found**: **C**, 33.95; **H**, 5.7; **N**, 45.3; **O**, 15.

3.2.1. Infrared analysis (FTIR)

FT-IR spectroscopy served as a pivotal analytical technique in elucidating the successful synthesis and subsequent structural modifications of the PVC-urea chelating composite. A comprehensive spectral analysis enabled the identification of key functional groups and provided compelling evidence for the urea condensation reaction with PVC. Characteristic vibrational modes associated with the unmodified PVC matrix were readily apparent, including prominent absorptions at 2846, 2908, and 2962 cm^{-1}, attributable to aliphatic -CH stretching, and peaks at 493 and 424 cm^{-1}, symptomatic of -C-Cl vibrations. Following the urea condensation, the FT-IR spectra exhibited the emergence of distinct and well-defined bands, confirming the formation of the PVC-urea derivative. Notably, new absorptions at 3209 and 3255 cm^{-1} were watched, relating to -NH stretching vibrations, alongside signals at 3417 cm^{-1} (-OH), 1249 cm^{-1} (-C-N), 1743 cm^{-1} (-C=O), and 1095 cm^{-1} (-C-O). A primary focus was directed towards the vibrational signatures at 3417 cm^{-1} and 1743 cm^{-1}, assigned to the vicinal -OH and carbonyl groups, respectively, as these were hypothesized to be significantly altered upon U(VI) chelation. Indeed, post-chelation, the intensities of these bands were diminished, and a discernible shift towards lower frequencies (approximately 15-25 cm^{-1}) was observed across the remaining spectral features. The appearance of novel bands at 609, 964, and 694 cm^{-1} in the chelated composite spectrum provides strong evidence for the formation of coordinate covalent bonds between U(VI) and oxygen atoms (-U-O), indicating successful chelation [37]. The FT-IR spectra illustrating these changes for PVC-urea and its U(VI) complex are presented in Figure 1.

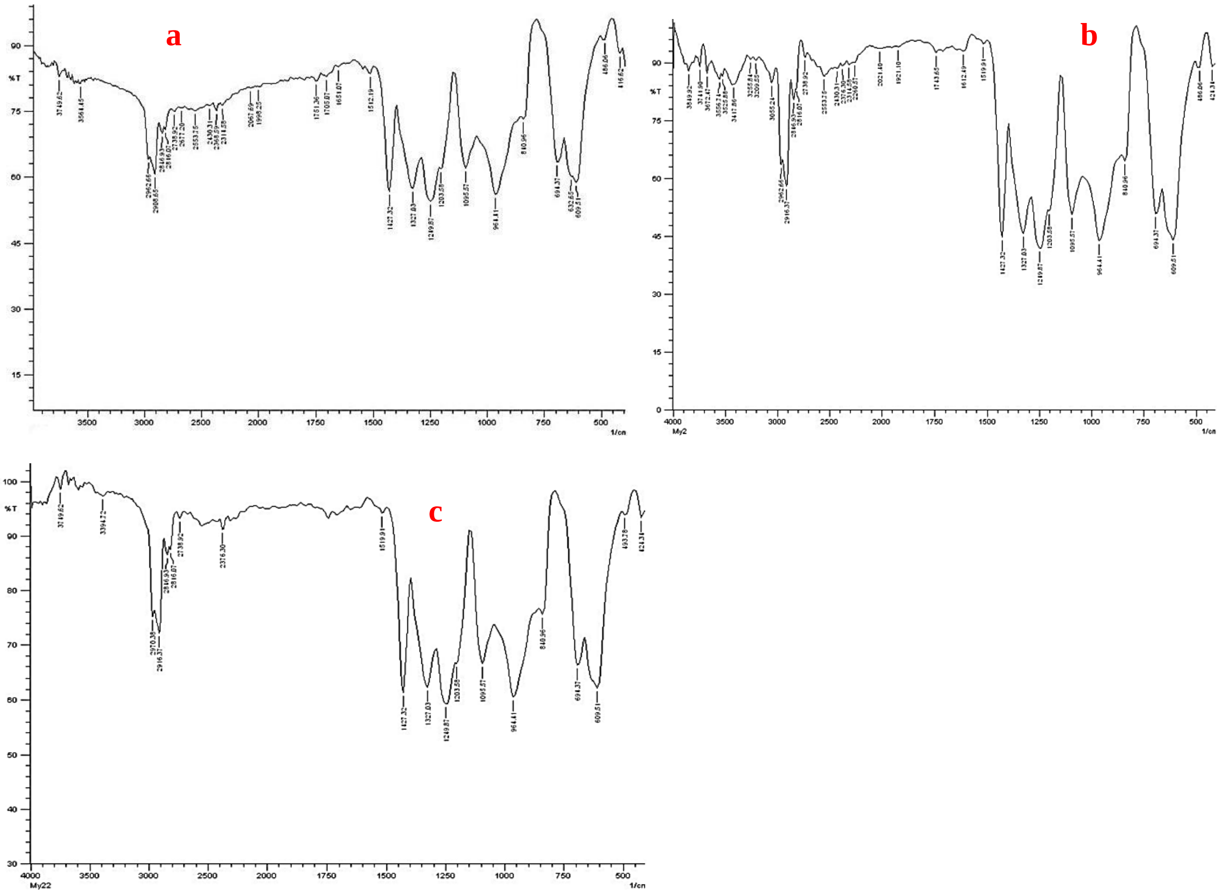

Figure 1.FTIR spectra of (a) unmodified PVC, (b) PVC-urea, (c) PVC-urea/U.

3.2.2. SEM-EDX analysis

SEM was employed to meticulously characterize the surface topographies of the PVC, PVC-urea, and PVC-urea/U materials, revealing initially uniform and pliable microstructures. Upon the condensation reaction transforming PVC into PVC-urea, a discernible alteration in surface morphology was observed, manifesting as a more discontinuous and heterogeneous texture. Subsequent institution of U(VI) ions to the PVC-urea matrix induced a significant transformation in the surface architecture, evolving into an intricate, tortuous network of microstructures characterized by enhanced surface roughness. This pronounced alteration is accredited to the effective sorption and integration of U(VI) onto the PVC-urea surface. Corroborating these morphological observations, EDX analysis provided definitive elemental composition verification, identifying the manifestation of C and Cl in PVC, C, Cl, O, and N in PVC-urea, and C, Cl, O, N, and U in PVC-urea/U. These findings collectively and unequivocally substantiate the successful synthesis of the PVC-urea chelating composite from PVC and, crucially, demonstrate its inherent capacity for the current sequestration of U(VI) ions, as visually represented in Figure 2a, b, and c.

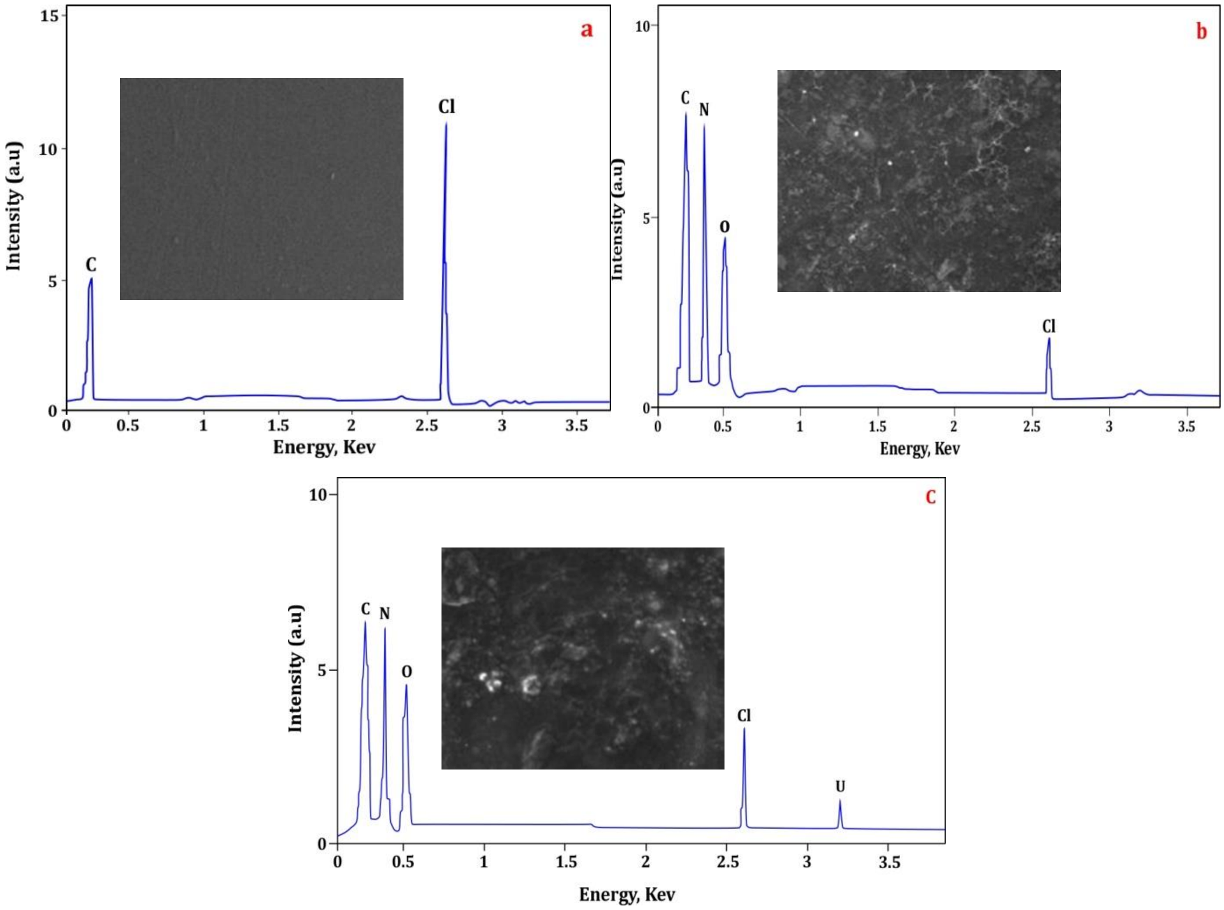

Figure 2.SEM-EDX of (a) PVC (b) PVC-urea (c) PVC-urea/U.

3.2.3. Thermal gravimetric analysis (TGA)

TGA was implemented to rigorously evaluate the impression of substance variation on the thermal stability of PVC combinations. Specifically, the thermal decomposition profiles of PVC, PVC-urea, and PVC-urea/U were meticulously characterized via TGA, with samples subjected to a controlled heating ramp from ambient temperature to 800 °C at a level of 10 °C/minute.

The consequential TGA thermographs, presented in Figure 3, reveal distinct stages of mass loss, characterized by deflection temperatures, percentage weight loss at each stage, and the final residual mass at the conclusion of the experiment (summarized in Table 4). Initial mass loss, up to 5% for all samples, was watched up to approximately 100 °C and is accredited to the volatilization of both physisorbed and chemisorbed water molecules, as supported by existing literature [38]. Post 100 °C, significant divergence in the decomposition behavior of neat PVC and the modified composites becomes apparent. The unmodified PVC exhibits three distinct inflection points, corresponding to temperature ranges of 100-250 °C (13% mass loss), 250-450 °C (64% mass loss), and 450-600 °C (12.5% mass loss), culminating in a 5.5% char residue at 600-800 °C. The substantial mass loss observed in the 250-450 °C range is attributed to the dehydrochlorination of the PVC polymer, resulting in the liberation of HCl and the formation of polyene sequences via cyclization reactions. Subsequent degradation within the 450-600 °C is potentially linked to the carbonization process, while the final stage may reflect thermo-oxidative degradation [39].

Comparatively, PVC-urea presents four inflection points within the temperature ranges of 100-346 °C (12.65% loss), 346-452 °C (34.65% loss), 452-583 °C (41% loss), and a final residual mass loss of 6.7% at 583-800 °C, which may be ascribed to the increasing in the organic components which represents the urea moiety. Similarly, PVC-urea/U displays four distinct degradation stages at 100-400 °C (12.73% loss), 400-500 °C (10.27% loss), 500-694 °C (62% loss), and an ending elevated weight char step of 10%, potentially arising from the construction of lasting uranium oxide in conjunction with the carbonaceous deposit. The observed shift in degradation temperature to 346 °C for PVC-urea, exceeding that of neat PVC, and an extra shift to 400 °C for PVC-urea/U, advanced than PVC-urea, strongly suggests the efficacious incorporation of U(VI) into the PVC-urea matrix, resulting in enhanced thermal stability [40].

Table 4.TGA assets PVC, PVC-urea and PVC-urea/U combinations.

Samples	PVC		PVC-urea		PVC-urea/U	
TGA stages	temp., ºC	wt loss, %	temp., ºC	wt loss, %	temp., ºC	wt loss, %
1st	0-100	5	0-100	5	0-100	5
2nd	100-250	13	100-346	12.65	100-400	12.73
3rd	250-450	64	346-452	34.65	400-500	10.27
4th	450-600	12.5	452-583	41	500-694	62
Final residue	600-800	5.5	583-800	6.7	694-800	10

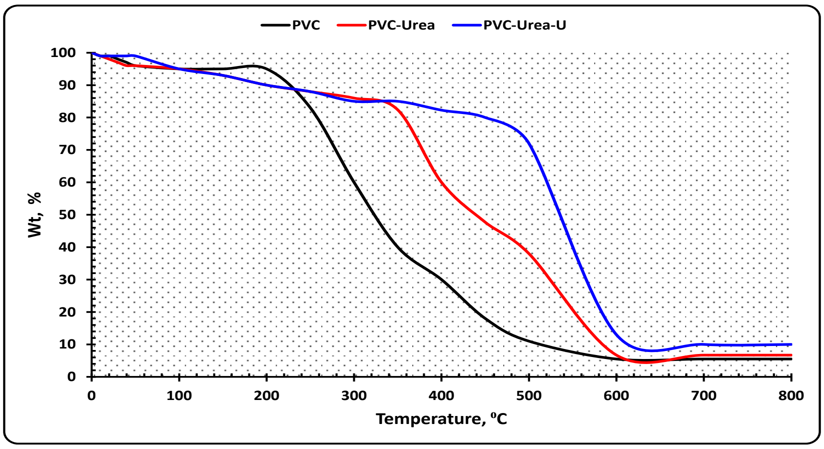

Figure 3.TGA of PVC, PVC-urea, and PVC-urea/U in a nitrogen situation.

3.2.4. ^{1}H-NMR analysis.

One useful tool for predicting the structure of the manufactured PVC-urea composite is ^{1}H-NMR analysis, which, at 25 °C, uses DMSO-d_6 as a solvent and tetramethyl silane as an authorized specimen. The analysis provides substantial documents viewing the protons in the composite. The primary δ (ppm) measurements for the original PVC foremost skeleton were recorded at 1.74, corresponding to $(-CH_2)_n$, while the other two measurements were recorded at 4.1 and 3.87, equivalent to the methine group linked to the chloride atom $(-CH)_n$-Cl and second methine group coupled to the urea moiety $(-CH)_n$-NH-CO-NH_2. The methine proton, when directly bound to the electronegative chlorine atom, is less insulated than the typical methylene group, and the chemical shift of the methine group linked to the urea mediety $(-CH)_n$-NH-CO-NH_2 is higher than that of the standard methylene group. These outcomes approve that urea incompletely amination altered the PVC. Branching PVC functionalized with urea has supplementary elementary δ (ppm) homework at 6.07 and 5.67 ppm, corresponding to one nitrogen proton (-NH) and two other nitrogen proton $(-NH_2)$ concurrent to a carbonyl group, respectively. It was anticipated that the presence of several proton assignments would reflect the composite's asymmetry caused by partial functionalization. For the reason that there are seven protons in the entire, the combination analysis also showings that there are two evident building blocks, $(CH_2\text{-}CHCl)_n$ and $(CH_2\text{-}CHNH\text{-}CO\text{-}NH_2)_n$. Figure 4 shows the results of the ^{1}H-NMR analysis of the PVC-urea composite.

3.2.5. ^{13}C-NMR analysis

Using DMSO-d_6 as a solvent and an energy of 100.04 MHz, the ^{13}C-NMR analysis provides valuable information regarding the carbon atom count in the produced PVC-urea composite. Methine carbon, $-(CH\text{-}Cl)_n$, methylene carbon, $(-CH_2)_n$, and $-(CH\text{-}NH\text{-})_n$ are associated with the foremost skeleton of the remaining unaltered PVC, which has main δ (ppm) at 55, 45.65, and 44.15 ppm as singlets. One potential justification for the significant magnitude of the carbonyl carbon chemical shift (-C=O, 159.09 ppm) is the functionalization caused by the urea moiety. Figure 5 guides the discoveries of the ^{13}C-NMR exploration of the PVC-urea combination.

3.2.6. Mass analysis (MS)

By GC/MS, the more stable fragment's base peak and the molecular formula's quasi-molecular ion highest can be predicted. The molecular weight of the produced PVC-urea $(-CH_2\text{-}CHNHCONH_2)_{n=1}$ building block is exemplified by the quasi-molecular ion highest, which has assessment of 106 and a qualified abundance of 18%. Roughly vital fragmentation structures that have been linked to the created PVC-urea combined have been branded, counting $[C_2H_3Cl]_{n=1}^{\cdot}$ with m/z=62 and an average abundance of 12%, which resembles to the vinyl chloride component, $[C_6H_5Cl]_{n=1}^{\cdot}$ with m/z=112 and an in relation abundance of 19%, which is associated to the chloro-benzene component, $[C_6H_4Cl_2]_{n=1}^{\cdot}$ with m/z=147 and an in relation abundance of 15%, which is associated to the dichloro-benzene component, $[C_2H_5N]_n=1^{\cdot}$ with m/z=43 and an in relation abundance of 30%, which is associated to vinyl amine component, that corresponds to good PVC amination. Together, these findings prove that the PVC-urea composite chain still contains vinyl chloride building blocks. Moreover, additional pieces were found that were thought to be indicators of the effective creation of PVC-urea, including $[NH_3]^{\cdot}$ with a m/z=17 and an approximate abundance of 95%, $[HCl]^{\cdot}$ with a m/z=36 and an in relation abundance of 99%, and $[CO_2]^{\cdot}$ with a m/z=44 and an in relation abundance of 85%, all of which are associated with CO_2 gas.

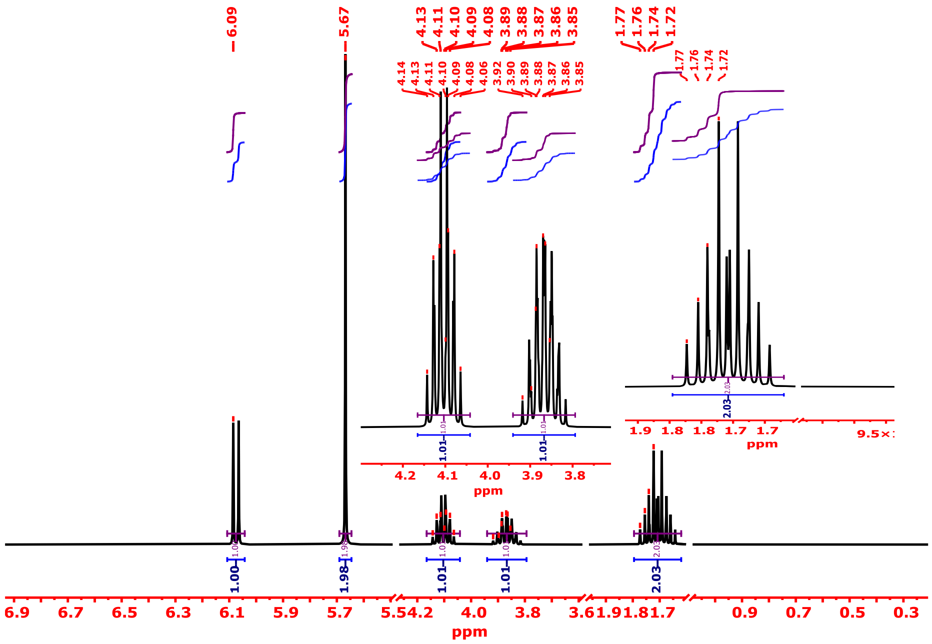

Figure 4. Specification of PVC-urea chelating composite by ^{1}H-NMR Spectrometry.

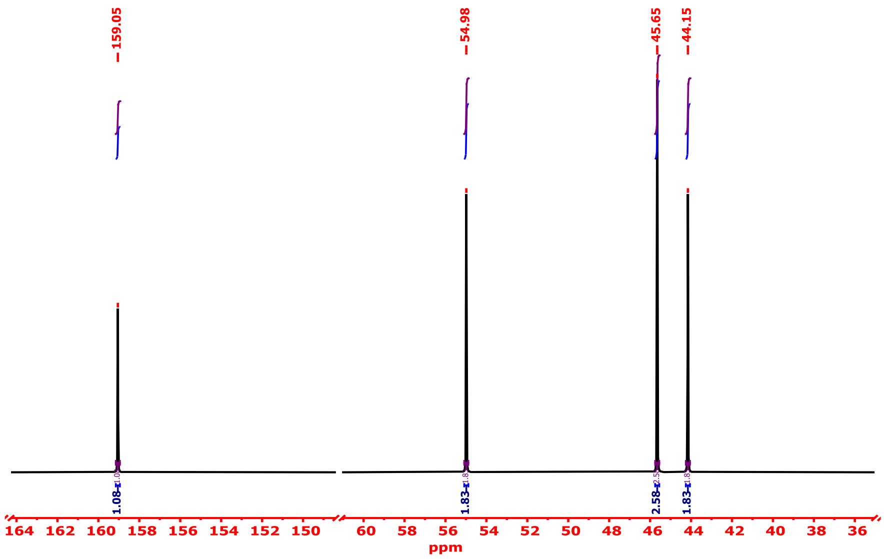

Figure 5. Specification of PVC-urea chelating composite by ^{13}C-NMR Spectrometry.

It is widely recognized that when PVC-urea undergoes exposure to an electron flux, HCl m/z=36 with an approximate abundance of 99% flows out, creating the polymerizing polyene, replaced polyenes, aromatics, and cooled aromatics, which can form cyclic molecules including benzene $[C_6H_6]^{\cdot}$with m/z=78 and an in relation abundance of 89%, naphthalene $[C_{10}H_8]^{\cdot}$with m/z=128 and an in relation abundance of 27%, anthracene $[C_{14}H_{10}]^{\cdot}$with m/z=178 and an in relation abundance of 11% and diamino naphthalene $[C_{10}H_{10}N]^{\cdot}$with m/z=158 and an in relation abundance of 25%. The results of the full investigation clearly indicate that the PVC-urea composite synthesis will be satisfactory. As seen in Figure 6, PVC-urea is described using GC/MS.

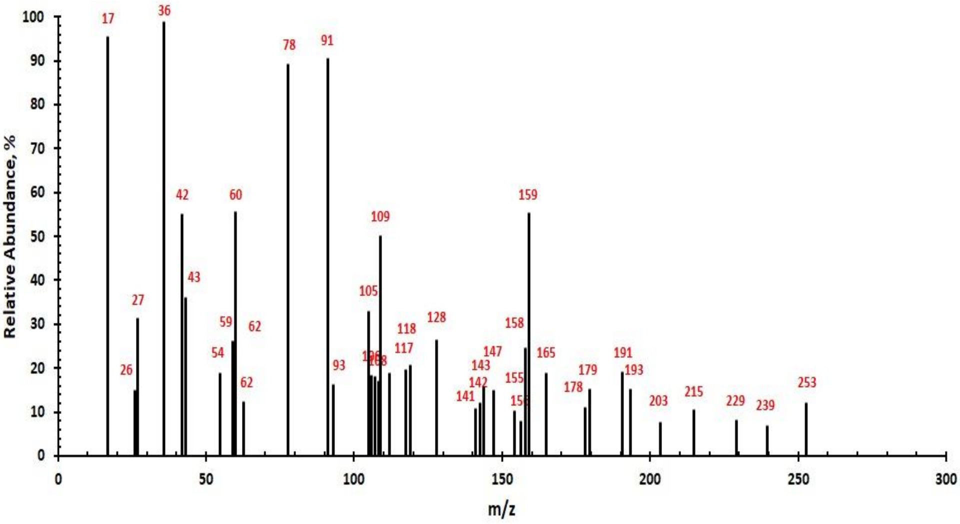

Figure 6. Specification of PVC-urea by Mass Spectrometry.

3.3. Adsorption prospects

3.3.1. The effect of pH

The pH environment critically governs the retention of UO_2^{2+} by the PVC-urea composite, exerting a multifaceted influence on both the aqueous speciation of uranium(VI) and the interfacial properties of the composite material [41]. In a controlled batch adsorption study, the efficacy of the PVC-urea composite for U(VI) retention was investigated across a pH range of 1 to 5, utilizing 25 mL of a 150 mg/L U(VI) solution and 0.05 g of the composite at ambient temperature, with an equilibration time of 5 minutes. As illustrated in Figure 7a, negligible U(VI) retention was observed under highly acidic conditions (pH 1-2), attributable to the protonation of the lone pair electrons on the composite's active sites, thereby diminishing their affinity for UO_2^{2+}. Subsequently, an incremental increase in U(VI) retention was observed with increasing pH from 2.5 to 5, correlating with partial deprotonation of the active sites and a concomitant enhancement of their binding capacity. Maximum U(VI) retention (Q_{max} = 19 mg/g) was achieved at pH 4.5, beyond which no significant improvement was noted, thus establishing pH 4.5 as the empirically determined optimum pH for U(VI) retention on the PVC-urea composite.

Furthermore, acknowledging the propensity of UO_2^{2+} to precipitate in the pH range of 3-4, the study considered the necessity of employing a solubilizing agent, such as citrate, to maintain uranium(VI) in solution. Spectroscopic characterization via ultraviolet-visible spectroscopy, coupled with speciation modeling, revealed that in citrate media, uranium(VI) exists as a complex mixture of UO_2^{2+}, $[UO_2Cit]^-$, and $[(UO_2)_2Cit_2]^{2-}$ species within the pH range of 2-3. At slightly higher pH values (3-7), the formation of polymeric complexes, potentially $[(UO_2)_3Cit_3]^{3-}$ and $[(UO_2)_6Cit_6(OH)_{10}]^{6-}$, was indicated. Literature suggests that such polymerization impedes the reduction of UO_2^{2+} in the presence of citric acid [42]. A ligand exchange mechanism is hypothesized, wherein uranyl citrate complexes undergo an exchange reaction with the PVC-urea composite, resulting in the chelation of UO_2^{2+} by the urea moieties of the composite and the concomitant release of citrate ions into the aqueous phase [43].

Quantitative analysis via linear regression of the distribution coefficient (log D) against pH yielded a linear relationship characterized by a slope of 1.987 and an intercept of 9.184 (Figure 7b). The slope value indicates the stoichiometric release of approximately two moles of hydrogen ions throughout the realization of the PVC-urea/U, consistent with a chelation process. Based on these findings, the stability constant (Log β) of the PVC-urea/U was intended at the optimum pH of 4.5, yielding a value of 9.1844. These results collectively underscore the complex interplay of pH-dependent factors governing U(VI) retention by the PVC-urea composite, supporting valued perceptions into the causing mechanisms and optimizing the performance of the composite material.

3.3.2. The effect of time of shaking

From an economic viewpoint, agitation time represents a critical operational parameter influencing the efficacy of U(VI) ion capture. To optimize this parameter, a rigorous investigation was undertaken to assess the impact of agitation duration, ranging from 2 to 60 minutes, on the uptake of U(VI) ions utilizing a 0.05 g PVC-urea composite in contact with 25 mL of a 0.63×10^{-3} mol/L (150 mg/L) aqueous uranium solution maintained at a pH of 4.5. As delineated in Figure 8a, the experimental results demonstrate a positive correlation between agitation time and the quantity of U(VI) ions adsorbed, culminating in a maximum uptake capacity at 10 minutes. This optimal agitation period yielded an adsorption capacity of 25 mg/g, corresponding to a 33.3% removal efficiency. Beyond this 10 minute threshold, the adsorption rate plateaus, indicating that equilibrium is effectively achieved. Consequently, considering both economic efficiency and process effectiveness, an agitation time of 10 minutes was determined to be sufficient for reaching equilibrium and was therefore adopted as the standard agitation duration for subsequent experimentation, thereby highlighting the favorable kinetic properties of the PVC-urea composite material for U(VI) ion removal.

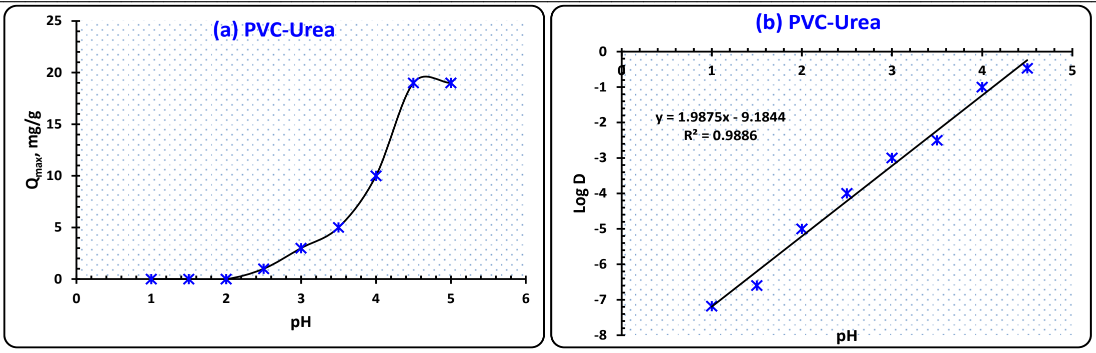

Figure 7.(a) The influence of pH on U(VI) retaining by PVC-urea (b) The slope regression assessment graph for U(VI) ions retaining by PVC-urea at altered pH ***(conditions:*** *25 mL, 150 mg/L U(VI), 0.05 g, 25°C, min).*

3.3.2.1. Kinetic features

Understanding the adsorption kinetics governing the uptake of U(VI) ions onto the PVC-urea composite material is paramount for elucidating the rate-determining steps in the overall sequestration process. Precisely defined kinetic parameters are indispensable, enabling accurate predictions of adsorption rates under varying operational conditions and providing fundamental data critical for the rational design and sophisticated modeling of optimized adsorption procedures. To comprehensively evaluate the mechanism underlying U(VI) ion adsorption onto the PVC-urea composite, pseudo-first order, pseudo-second order, and intra-particulate diffusion kinetic models were rigorously applied. Subsequent analysis facilitated the estimation of the rate constants associated with each stage of the adsorption process, providing valuable insights into the relative contributions of surface adsorption, diffusion, and chemical reaction phenomena. The derived pseudo-first-order kinetic model, as mathematically defined by Eq. 3 and previously detailed in reference [44], serves as a foundational element for quantifying the initial stages of U(VI) adsorption and projecting performance under specific experimental scenarios.

$$Log\,(q_e - q_t) = Logq_e - (\frac{K_1}{2.303})t \quad \text{....................(3)}$$

First-order kinetic modeling was applied to elucidate the adsorption dynamics of U(VI) ions. Linear regression analysis, as depicted in Figure 8b, utilizing a design of Log(q_e-q_t) versus time, facilitated the determination of the pseudo-first-order adsorption rate constant (K_1) and the balance adsorption capability (q_e) through examination of the resulting slope and intercept, respectively. The calculated equilibrium adsorption capacity, derived from this analysis, was determined to be 25.35 mg/g, demonstrating a high degree of concordance with the empirically observed value of 25 mg/g. Furthermore, a compelling adsorption rate constant of 0.548 min^{-1} (K_1 = 0.548 min^{-1}), coupled with a robust coefficient of determination (R^2 = 0.9961), strongly suggests that the pseudo-first-order provides a statistically significant and representative fit for the experimental data, accurately capturing the temporal evolution of U(VI) adsorption within the studied system.

The kinetic modelling of the pseudo-second-order is named manipulating the next Eq. 4 [45]:

$$\frac{t}{q_t} = \frac{1}{k_2 q_e^{\,2}} + (\frac{1}{q_e})t \quad \text{.....................(4)}$$

The adherence of empirical data to the pseudo-second-order, as evidenced in Figure 8c, substantiates its utility in describing the adsorption process under investigation. Linear regression scrutiny of the t/qt plot yielded a slope of 1/qe and an intercept of $1/k_2q_e^2$, from which a theoretically derived balance adsorption capacity (q_e) of 25.31 mg/g was reckoned. This value exhibits a high degree of concordance with the experimentally determined uptake of 25 mg/g, further reinforced by a remarkably high correlation coefficient (R^2) of 0.9996 and an adsorption rate constant (k^2) of 0.037 g/mg.min. These findings compellingly demonstrate the applicability of the pseudo-second-order in accurately portraying the observed adsorption behavior, suggesting its suitability as a framework for elucidating the underlying mechanisms governing this system. Given the performance characteristics of both first and second-order kinetic models, the cumulative evidence suggests the potential for a mixed-order modeling approach to provide a more comprehensive and nuanced interpretation of the adsorption phenomena.

The adsorption of U(VI) onto PVC-urea is posited as a liquid-solid contact, wherein the kinetics of U(VI) ion uptake can be modulated by several interconnected phenomena operating at the interface. Specifically, the rate-limiting steps potentially encompass (1) bulk diffusion, governing the transport of U(VI) ions from the bulk solution to the hydrodynamic film surrounding the composite's active sites, (2) external diffusion, characterizing the inter-sphere migration of U(VI) ions within the solution proximate to the adsorbent surface, (3) intra-particle diffusion, representing the movement of U(VI) ions within the porous structure of the PVC-urea composite, and (4) a range of surface interaction mechanisms, including physisorption, chemisorption, ion exchange, and complexation, facilitating direct interaction concerning U(VI) ions and the available binding sites on the PVC-urea matrix [46].

The hydrodynamics of the system, particularly the agitation speed, exerts a significant influence on the external diffusion process and, consequently, the overall adsorption rate; increased agitation reduces the boundary layer thickness, thereby enhancing mass transfer. To elucidate the potential rate-controlling role of intra-particle diffusion, the Weber and Morris model was employed to analyze the temporal evolution of U(VI) adsorption, correlating uptake with the square root of time to assess the contribution of intra-particle transport in governing the overall U(VI) sorption kinetics onto the PVC-urea composite [47].

$$q_t = K_{ad}\sqrt{t} + I \quad \text{……………………(5)}$$

The kinetic analysis of U(VI) ion uptake by the PVC-urea composite material, predicated on intra-particle diffusion, revealed noteworthy insights into the adsorption mechanism. Specifically, the rate constant (K_{ad}), indicative of the adsorption velocity and derived from the linear relationship observed between qt (uptake capacity at time t) and $t^{1/2}$ (as depicted in Figure 8d), was quantified as 4.6685 mg/g min$^{-1/2}$. Furthermore, the calculated boundary layer thickness (I), a critical parameter influencing mass transfer resistance, was determined to be 11.472. The positive value of this parameter suggests a plausible rate-limiting role for intra-particle diffusion in the adsorption process. However, the relatively modest correlation coefficient ($R^2 = 0.8369$) associated with the linear fit necessitates a cautious interpretation of this finding and underscores the potential influence of other contributing factors. While these kinetic parameters, summarized comprehensively in Table 5, offer valuable insights into the U(VI) adsorption behavior, further investigation utilizing complementary kinetic models and analytical techniques is warranted to elucidate the complex interplay of mechanisms governing the overall adsorption process and to achieve a more robust understanding of the system's behavior.

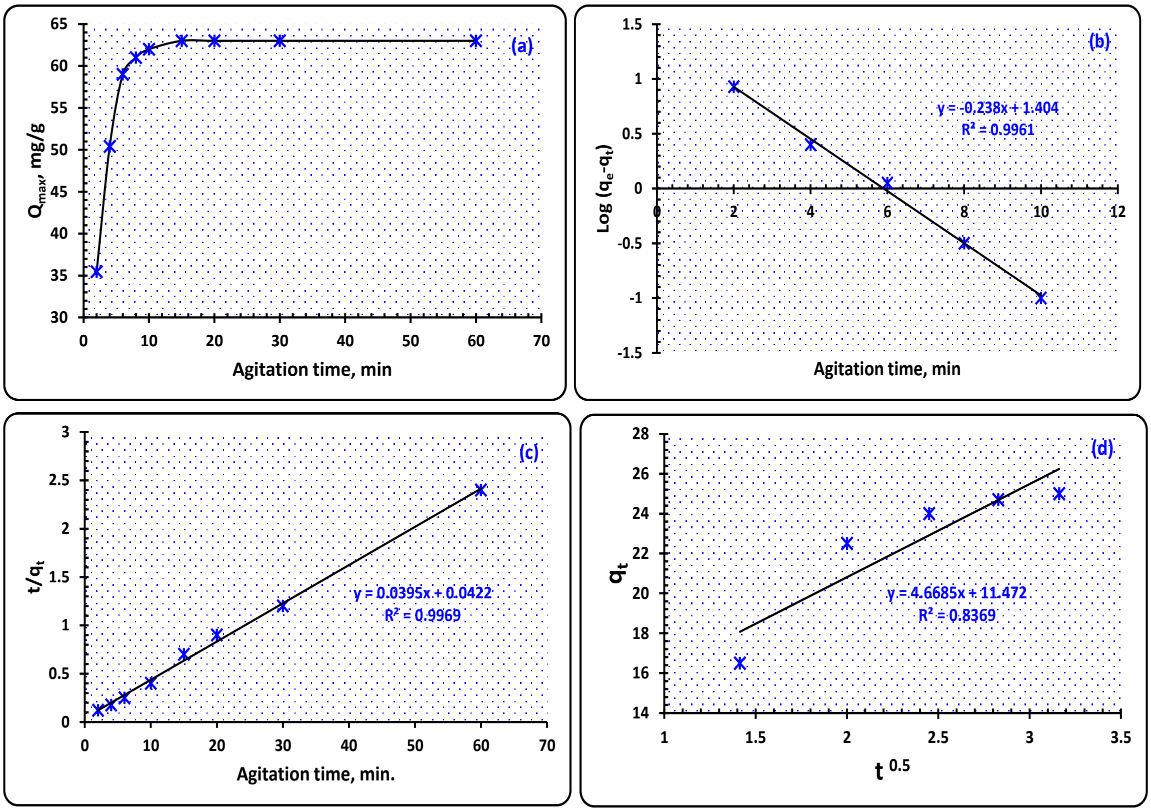

Figure 8.(a) Influence of shakeup time on U(VI) uptake by PVC-urea (b) Pseudo-first order modelling (c) Pseudo-second order modelling (d) Intra-particle diffusion modelling, ***(conditions:** 25 mL, 150 mg/L U(VI), pH4.5, 0.05 g, 25°C,).*

Table 5. Kinetic constraints of U(VI) sorption upon PVC-urea.

Exp. capacity q_{max}, mg/g	Pseudo-first order			Pseudo-second order			Intra-particle diffusion		
	q_e	K_1	R^2	q_e	K_2	R^2	K_{ad}	I	R^2
25 mg/g	25.35	0.548	0.9961	25.31	0.037	0.9969	4.668	11.472	0.8369

3.3.3. The impact of initial ions concentration

Investigating the influence of initial uranium concentration on its uptake is critical for influential the extreme adsorption ability and potential applicability of the PVC-urea composite material. The observed relationship, as illustrated in Figure 9a, exhibits a biphasic behavior. Initially, a marked increase in U(VI) uptake is evident within the concentration of 10 to 50 mg/L. This pronounced enhancement is attributed to the abundance of available active sites on the PVC-urea composite, which, at lower U(VI) concentrations, are not fully utilized due to the limited availability of uranyl ions. Consequently, the composite exhibits an elevated affinity for U(VI) and effectively sequesters the available ions. Subsequently, as the initial concentration grows from 50 to 200 mg/L, the U(VI) uptake plateaus, representative of the saturation of accessible required sites on the PVC-urea matrix. This saturation effect indicates that the composite's capacity to adsorb additional U(VI) ions is limited by the finite number of active sites. Under the experimental conditions, a maximum U(VI) uptake of approximately 25 mg/g was achieved at an initial concentration of 50 mg/L, demonstrating the optimal loading capacity of the PVC-urea composite at ambient temperature. This value provides a crucial benchmark for assessing the material's performance and scalability for potential uranium remediation applications.

3.3.3.1. Distribution isotherm modelling

To rigorously quantify the uranium(VI) ion adsorption behavior onto the PVC-urea composite, a comprehensive assessment of the accumulated U(VI) ions was performed, specifically correlating to the established equilibrium concentration at ambient temperature. The analysis employed the Langmuir adsorption isotherm, a theoretical framework predicated upon a set of well-defined criteria. These fundamental assumptions include: (a) the attainment of maximum adsorption capacity coinciding with the formation of a complete, saturated monolayer of adsorbate species upon the adsorbent surface; (b) a consistent and uniform adsorption energy profile across all binding sites, indicative of homogenous surface characteristics; and (c) the absence of lateral interactions or surface diffusion phenomena, ensuring that adsorbed molecules remain localized and independent. Consequently, the Langmuir isotherm model, mathematically expressed through the derived Eq. 6 [48, 49], provides a robust analytical tool for elucidating the underlying mechanisms governing the observed adsorption phenomenon.

$$\frac{C_e}{q_e} = \frac{1}{q_e b} + \frac{C_e}{q_e} \;\ldots\ldots\ldots\ldots\ldots\ldots\ldots(6)$$

Linearization of the equilibrium data allowed for a thorough evaluation of the U(VI) adsorption manner's adherence to the Langmuir isotherm model. In particular, the linear correlation between C_e/q_e (where q_e is the overall amount of U(VI) ions adsorbed at balance, and C_e is the balance concentration in mg/L) is shown in Figure 9b. This proves that the adsorption mechanism follows the Langmuir paradigm. An additional piece of evidence supporting this conclusion is the strong statistical fit indicated by the significant correlation coefficient ($R^2 = 0.99$) that was acquired from the linear regression assessment applied to the Langmuir plot. Langmuir constants, which are critical for describing the adsorption behavior, were found to be $q_e = 24.1$ mg/g and b = 3.1 L/mg, respectively, from the slope and intercept of this linear relationship. Important information about the adsorbent-U(VI) ion interaction can be gleaned from these parameters, which stand for the maximum adsorbed capability (q_e) and the adsorption energy (b), respectively. This particular adsorption process can be accurately and reliably described by the Langmuir model since the computed q_e value agrees closely with the practically reported adsorption capability of 25 mg/g. In order to gain a better grasp of the adsorption efficiency and feasibility under different experimental conditions, one can use the dimensionless separation factor, also renowned as the balance parameter (R_L), as defined by Eq. 7 [50], to shed light on the basic assets of the Langmuir isotherm.

$$R_L = \frac{1}{1+bC_o} \;\ldots\ldots\ldots\ldots\ldots\ldots\ldots\ldots(7)$$

Here, b is the value of the Langmuir constant, and C_o is the starting concentration of U(VI) ions, which can be anywhere from 10 to 200 mg/L. The conclusions steered that the PVC-urea had strong adsorption of U(VI) ions, with R_L values ranging from 0.0312 to 0.0016.

The Freundlich isotherm framework was also employed for the adsorption process [51]. Granting this equation is profoundly numerical, it is regularly helpful for explaining data. The Freundlich equilibrium model is shown by Eq. 8:

$$Log q_e = Log K_f + \left(\frac{1}{n}\right) Log C_e \;\ldots\ldots\ldots\ldots\ldots\ldots\ldots...(8)$$

An analysis of the equilibrium sorption pattern of U(VI) ions onto the produced PVC-urea was conducted using the Freundlich isotherm model. In this model, C_e is the balance content (mg/L), and q_e is the quantities of U(VI) ions adsorbed at balance. K_f, the Freundlich constant, and n, the adsorption intensity, are both determined by the linear regression of Log $q_e$vs Log C_e. These two variables stand for the adsorption uptake capability (mg/g) and the affinity. With a n value between 0 and 10, which is often associated with good adsorption properties, and a computed K_f value of 16.76 mg/g, the adsorption route appears to be going well. The Freundlich plot showed a strong correlation (R^2= 0.9992), indicating that the model fits well. However, as shown in Figure 9c, the experimentally calculated adsorption capacity was superior than the observed K_f value (16.76 mg/g). This difference suggests that, in this particular case, the experimental data may be better captured by the Langmuir isotherm concept than by the Freundlich model. Table 6 provides an extensive summary of the adsorption characteristics obtained from the examination of U(VI) sorption onto the PVC-urea, including a comprehensive review of the isotherm parameters.

Table 6. Isotherm considerations of U(VI) adsorption upon PVC-urea composite.

Exp. capacity q_{max}, mg/g	Langmuir model			Freundlich model		
	q_e	b	R^2	K_f	n	R^2
25 mg/g	24.1	3.1	0.99	16.76	1.873	0.9992

3.3.4. The effect of PVC-urea dose

To elucidate the effect of PVC-urea dosage on uranium uptake, a systematic investigation was conducted to evaluate the influence of varying composite concentrations (0.01 g to 0.5 g) on the adsorption of U(VI) ions under a persistent U(VI) concentration of 50 mg/L. This concentration corresponds to the experimentally determined maximum uptake capacity of 25 mg/g achieved with a 0.05 g dose of the PVC-urea composite. Analysis of the data, as depicted in Figure 9d, reveals a nuanced relationship: initial augmentation of the composite dosage from 0.01-0.05 g resulted in a commensurate augment in U(VI) ion uptake. However, subsequent escalation of the dosage beyond 0.05 g induced a gradual decline in uptake efficiency. This phenomenon is attributed to a saturation effect, wherein the introduction of excess composite material surpasses the available U(VI) ions, leading to a surplus of unoccupied active binding sites. Specifically, expanding the composite dose from 0.05-0.5 g caused a demonstrable reduction in U(VI) uptake, as the abundance of active sites on the composite far exceeded the concentration of U(VI) in the solution. Consequently, these findings suggest that a composite dose of 0.05 g represents an optimal threshold, yielding a superlative uptake capability of 25 mg/g, effectively sequestering the equivalent of 50 mg/L U(VI) ions, thereby highlighting its potential for uranium remediation applications.

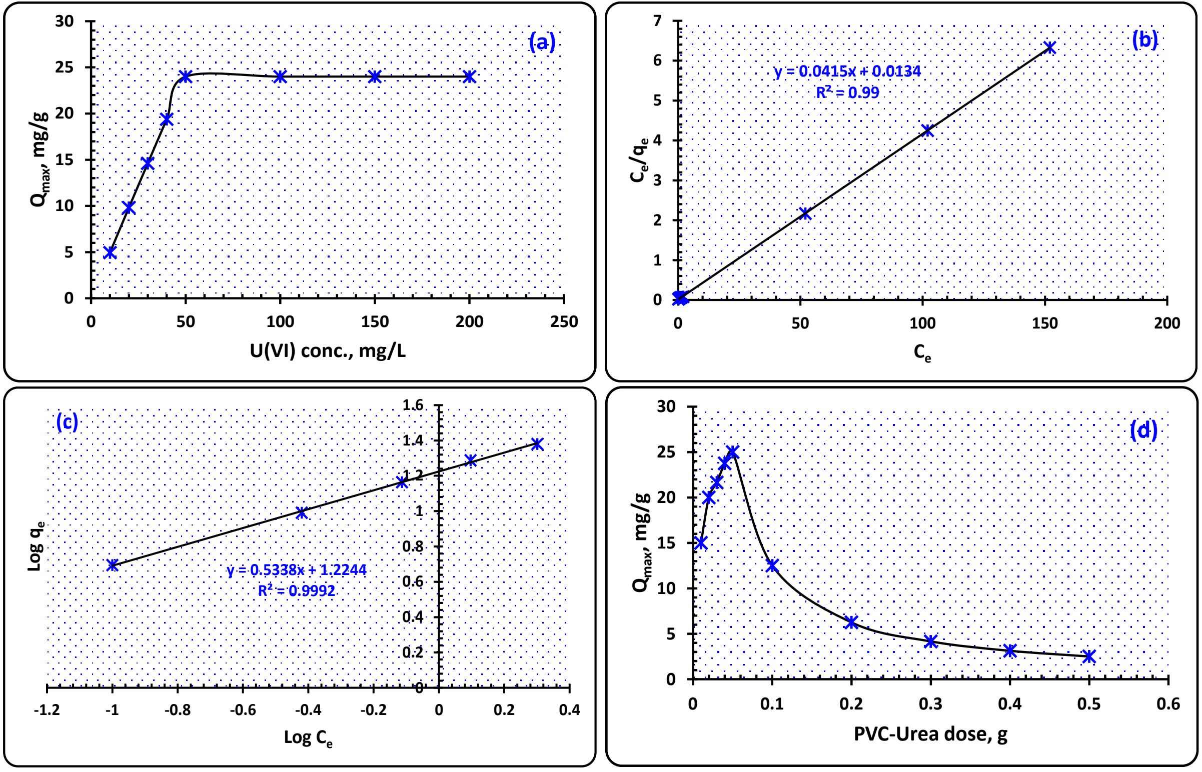

Figure 9.(a) Influence of initial U(VI) conc. on uptake by PVC-urea (b) Langmuir isotherm modeling (c) Freundlich isotherm modelling (d) Influence of PVC-urea dose on U(VI) uptake, ***(conditions:** 25 mL, 0.05 g, 25°C, pH4.5, 150 mg/L U(VI), 10 min).*

3.3.5. Thermodynamic features

Thermodynamic analysis, leveraging both Van't Hoff and Gibbs free energy calculations, provides a robust framework for elucidating the influence of temperature on adsorption equilibrium and the spontaneity of uranium(VI) ion adsorption processes. To investigate this effect, a series of controlled experiments were conducted, wherein 0.05 g of a PVC-urea composite material was brought into contact with 25 mL of an aqueous uranium solution, maintained at a concentration of 150 mg/L and a pH of 4.5, for a duration of 10 minutes. The temperature was systematically varied between 298 K and 353 K, allowing for a comprehensive assessment of its impact on uranium uptake. Quantifiable results revealed a discernible inverse relationship between temperature and uptake capacity; specifically, an elevation in temperature from 298 to 353 K correlated with a reduction in uptake capacity from 25 mg/g to 15 mg/g respectively. This temperature-dependent behavior, visually represented in Figure 10a, strongly suggests that the adsorption of uranium(VI) ions onto the PVC-urea composite is an exothermic process, indicative of a process that releases heat as adsorption occurs.

To estimate thermodynamic variables, including Gibbs free energy (ΔG, kJ/mol), enthalpy change (ΔH, kJ/mol), and entropy change (ΔS, J/mol.K). The following equations [52] were used to measure these thermodynamic limitations:

$$\Delta G = -2.303RTLogK_d \text{ ....(9)}$$

$$LogK_d = \frac{\Delta S}{2.303R} - \frac{\Delta H}{2.303RT} \text{ ....(10)}$$

Utilizing the Van't Hoff equation and leveraging the fundamental relationship between the equilibrium constant (K_d) and thermodynamic parameters, the experimental data, as visually depicted in Figure 10b, provides compelling evidence for the precise determination of both the enthalpy change (ΔH) and entropy change (ΔS) associated with the process under investigation. Specifically, through rigorous linear regression analysis of the plot of Log K_d versus the reciprocal of absolute temperature (1/T), where T is expressed in Kelvin and R (8.314 $J.mol^{-1}.K^{-1}$) signifies the universal gas constant, a definitive linear correlation has been established. The derived slope of 554.27 and y-intercept of -2.4656, obtained from this analysis, serve as critical values for the accurate quantification of ΔH and ΔS, respectively, enabling a comprehensive thermodynamic characterization. The exceptionally high correlation coefficient ($R^2 = 0.9937$) further validates the robustness and reliability of the experimental data and the subsequent thermodynamic calculations, reinforcing the significance of this approach for determining these crucial thermodynamic properties.

The exothermic nature of U(VI) ion adsorption onto the PVC-urea composite, as evidenced by the negative enthalpy change (ΔH = -10.62 kJ/mol) documented in Table 7, underscores a process wherein heat is liberated during the binding interaction. The marginal decrease in entropy (ΔS = -0.0472 kJ/mol) suggests a limited reduction in the system's degrees of freedom upon adsorption, potentially attributable to restricted mobility of the U(VI) ions upon immobilization on the composite matrix. Furthermore, the positive Gibbs free energy (ΔG) values indicate that, under standard conditions, the adsorption process is thermodynamically unfavorable, exhibiting a temperature-dependent spontaneity. Specifically, the escalation of ΔG values from 3.434 kJ/mol at 298 K to 6.1 kJ/mol at 353 K implies a preferential adsorption affinity at lower temperatures. Finally, the Arrhenius equation, leveraged through the linear relationship observed in Figure 10b, serves as a critical tool for determining the apparent activation energy (E_a) governing U(VI) ion adsorption onto the PVC-urea composite, with the mathematical formalism for its calculation readily available in established literature as in Eq. 11 [53].

$$LogK_d = \frac{-2.303E_a}{RT} + LogA \text{ ....(11)}$$

The partitioning behavior of U(VI) ions onto the PVC-urea composite material is governed by a thermodynamically favorable adsorption process characterized by a negative adsorption activation energy (E_a) of -2 kJ/mol. This value, incorporated within the broader context of the partition coefficient (K_d) equation, where K_d is functionally related to the pre-exponential factor (A), the gas constant (R), and absolute temperature (T) in Kelvin, indicates a spontaneous and exothermic interaction. The negative E_a signifies that the adsorption of U(VI) onto the composite releases energy, proceeding favorably without the necessity for external energy input. Consequently, the adsorption equilibrium exhibits a relatively low sensitivity to temperature variations, suggesting a process primarily driven by inherent thermodynamic factors rather than kinetic limitations imposed by thermal energy. This implies that the composite material demonstrates a robust affinity for U(VI) ions even under ambient temperature conditions.

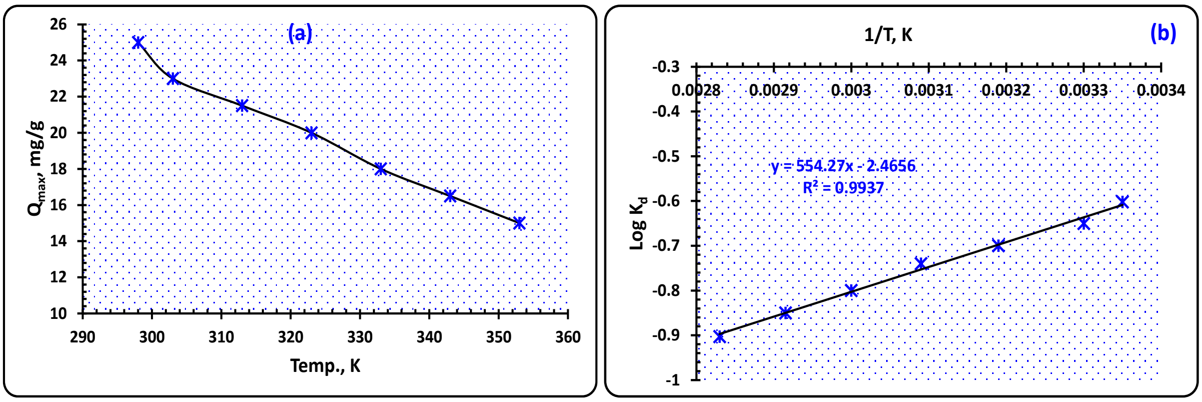

Figure 10.(a) The consequence of temperature on U(VI) uptake by PVC-urea, (b) The consequence of temperature on the partition coefficient of U(VI) applying PVC-urea.

Table 7. The thermodynamic indicators of U(VI) sorption upon PVC-urea.

Parameter	ΔH, kJ/mol	ΔS, kJ/mol.K	ΔG, kJ/mol						
			298 K	303 K	313 K	323 K	333 K	343 K	353 K
U(VI)	-10.62	-0.0472	3.43	3.77	4.19	4.57	5.1	5.58	6.1

3.3.6. The effect of co-existing ions

The investigation of the leach liquor revealed the presence of several co-ions alongside U(VI), necessitating a comprehensive evaluation of their potential influence on the adsorption process. To ascertain the impact of these co-existing ions under optimized adsorption conditions, individual ions were introduced into 25 mL aliquots of a 150 mg/L U(VI) solution. A co-ion was classified as an interfering species if the resultant uranium adsorption percentage deviated by more than ± 3% from the control. The tolerance limit, defining the permissible concentration of each interfering ion, was established as the concentration that induced a uranium adsorption error exceeding the ± 3% threshold. Analysis of the data presented in Table 8 demonstrates that specific co-ions, including Fe^{3+}, Ni^{2+}, Pb^{2+}, Zr^{4+}, Mn^{2+}, and Zn^{2+}, exerted a discernible inhibitory effect on the U(VI) adsorption efficiency of the PVC-urea composite. Conversely, the remaining co-ions tested exhibited no statistically significant impact on U(VI) adsorption. These findings underscore the notable selectivity of the PVC-urea composite for U(VI), suggesting its potential applicability for targeted uranium extraction from complex leach liquors containing a diverse range of co-ionic species.

Table 8. The effect of co-ions upon U(VI) adsorption using PVC-urea.

Co-ions	Tolerance limit*, mg/L	U(VI) adsorption %	Co-ions	Tolerance limit*, mg/L	U(VI) adsorption %
Na$^+$	1000	99.9	Ba^{2+}	1000	99.9
K$^+$	1000	99.9	Ni^{2+}	700	97
Si^{4+}	1000	99.9	Rb$^+$	1000	99.9
Al^{3+}	1000	99.9	Pb^{2+}	800	97
Ca^{2+}	900	97	Mo^{6+}	950	97
Mg^{2+}	900	97	Zr^{4+}	800	97
Fe^{3+}	850	97	Sr^{2+}	975	97
P^{5+}	1000	99.9	Mn^{2+}	900	97
Ti^{4+}	975	97	Zn^{2+}	850	97

*(**Adsorption conditions:** pH: 4.5, V: 25 mL, m; 0.05 g, Agitation time: 10 min., U (VI): 150 mg/L, temp. : 25 ˚C˚)*

** **Tolerance limit:** the conc. of co-ion that cause an error in U(VI) adsorption efficiency not exceed ± 3%.*

3.3.7. Uranium elution

To optimize the back-adsorption, or elution, of U(VI) from the PVC-urea composite, a rigorous evaluation was conducted utilizing three mineral acids – nitric acid (HNO_3), hydrochloric acid (HCl), and sulfuric acid (H_2SO_4) – at varying concentrations ranging from 0.025-2 M. This study, performed at ambient temperature, employed a standardized protocol of 10 mL of eluting agent per 0.05 g of U(VI)-loaded PVC-urea composite. The data presented in Table 9 unequivocally demonstrates a direct correlation between acid concentration and U(VI) elution efficiency. Specifically, lower acidic concentrations exhibited diminished elution capabilities, while elevated concentrations significantly enhanced the recovery of U(VI). Notably, near-quantitative elution efficiencies of 99% were ensued utilizing 0.5 M HNO_3, 0.5 M HCl, and 1 M H_2SO_4. While all three acids demonstrated exceptional efficacy, the economic viability of employing 0.5 M H_2SO_4 warrants serious consideration for large-scale applications, suggesting a potentially cost-effective solution without compromising performance. Further economic analysis should be conducted to confirm this preliminary assessment.

Table 9. Effect of eluting agents conc. on U(VI) elution from loaded PVC-urea composite.

Acid conc., (M)	Elution efficiency, (%)		
	HNO_3	HCl	H_2SO_4
0.025	60	50	45
0.05	85	67	65
0.1	95	80	90
0.5	99	99	97
1	99	99	99
2	99	99	99

A comparative study for different composites for UO_2^{2+} ionsadsorption is shown in Table 10.

Table 10. Uptake capacity of different composites for UO_2^{2+} ions.

Composites	Conditions	Q_{max}, mg/g	Ref.
polyamidoxime–phosphorylated cellulose (PAO-PCNF)	72 h, pH 5	27.1	[54]
Turbostratic boron nitride (tBN/Pin) nanoadsorbent	10 min., pH 5-5.5	315.29	[55]
gum-g-poly(AAm) composite	2 h, pH 6	367.65	[56]
MQ_2-collagen fibers ((MoS_2-CF)	12 h, pH 5	95.7	[57]
GGAmB Hydrogel Composite	2.5 h, pH 5.5	263.2	[58]
CH-S	25 min., pH 4	357	[59]
Fe-incorporated zeolite (BEA-Fe30)	26 h, pH 6	125	[60]
Kaolinite-titanium hydroxide composite	20 min. pH 5	205	[61]
PVC-urea		25	present study

3.3.8. Uranium adsorption from G.Gattar solution by PVC-urea composite

The efficacy of a new PVC-urea composite as an adsorbent for uranium(VI) from sulfate solutions has been definitively demonstrated. Building upon this foundation, the composite's performance was rigorously evaluated utilizing a synthetic G. Gattar solution, meticulously formulated to replicate the complex geochemical conditions of uranium leach liquors, specifically assaying at 0.45 g/L U(VI) and incorporating a representative suite of metallic impurities. Employing a scaled experimental design under previously optimized parameters – specifically, a 3 L volume of the synthetic leach liquor treated with 10g of the PVC-urea composite under controlled conditions (pH 4.5, 10-minute agitation period, and a consistent temperature of 25°C) – a remarkable 99% uranium(VI) adsorption efficiency was achieved. Furthermore, subsequent elution studies unequivocally confirmed the facile recovery of adsorbed uranium(VI) through the application of a 1M sulfuric acid solution, highlighting the potential for cost-effective and efficient uranium recovery processes leveraging this innovative PVC-urea composite material. This establishes the composite as a promising candidate for selective uranium extraction from complex aqueous matrices.

4. Conclusion

A proficient synthesis of a urea-modified polyvinyl chloride (PVC) composite has been achieved, demonstrating its efficacy in the elimination of U(VI) in leach solution. The synthesized composite was comprehensively characterized using a suite of analytical techniques. The static adsorption process was meticulously optimized, establishing an ideal configuration consisting of a 25 mL solution encompassing 150 mg/L of U(VI), disturbed with 0.05 g of the PVC-urea composite at a pH of 4.5 for a duration of 10 minutes. In these optimized constraints, the made composite unveiled a utmost U(VI) uptake ability of 25 mg/g at 25 °C. Linear regression scrutiny, purposely slope analysis derived from a plot of log D versus pH, yielded a linear relationship with a slope of 1.9785, indicating the release of approximately two moles of hydrogen ions into the solution during adsorption. Furthermore, a high stability constant ($\log \beta = 9.1844$) for the PVC-urea/U complex was determined at the optimal pH of 4.5.

Kinetic modelling statistics suggest a mixed pseudo-first and second-order model best describes the adsorption behavior, with theoretical uptake values of 25.35 mg/g and 25.31 mg/g, respectively, closely aligning with the experimentally observed value of 25 mg/g. The positive value obtained for the boundary layer thickness (I), coupled with a low correlation coefficient ($R^2 = 0.8369$), implies that intra-particle diffusion does not serve as the rate-limiting step in the U(VI) ion adsorption onto the PVC-urea composite.

Evaluation of distribution isotherm models revealed the Langmuir model to be the most suitable representation of the retaining system, yielding an uptake rate of 24.1 mg/g, which closely approximates the experimental value. Thermodynamic analysis indicated the adsorption process to be exothermic, non-spontaneous, and ideal at lesser temperatures, as evidenced by the derived thermodynamic constraints: ΔS (-0.0472 kJ/mol), ΔH (-10.62 kJ/mol), and ΔG (ranging 3.43 - 6.1 kJ/mol at 298-353 K, representative growing non-spontaneity with rising temperature).

Efficient elution of U(VI) from the PVC-urea-U was drained using 0.5M H_2SO_4, with a recovery rate of 97%. The PVC-urea composite also demonstrated a commendable tolerance towards a wide range of co-existing ions in the solution, suggesting its potential for practical application in complex environmental matrices.

References

[1] **B.M. Atia,** 1,5-Diphenylthiocarbazone Modified Amberlite XAD-7: A chelating Collector for Upgrading Uranium Concentrate produced from G.Gattar pilot plant, North Eastern Desert, Egypt, Radiochemistry, 61(6), **2019**, 703-710.https://doi.org/10.1134/S1066362219060158.

[2] **B.M. Atia, M.A. Gado, M.F. Cheira,** Kinetics of Uranium and Iron Dissolution by Sulfuric Acid from Abu Zeneima ferruginous siltstone, Southwestern Sinai, Egypt, Euro-Mediterranean Journal for Environmental Integration, 3(39), **2018**, 1-12. https://doi.org/10.1007/s41207-018-0080-y.

[3] **M. Gado, B. Atia, A. Morcy,** The role of graphene oxide anchored 1-amino-2-naphthol- 4-sulphonic acid on the adsorption of uranyl ions from aqueous solution: kinetic and thermodynamic features, International Journal of Environmental Analytical Chemistry, **2019**, https://doi.org/10.1080/03067319.2019.1617283.

[4] **M.E. Khalifa,** Selective separation of uranium using Alizarin Red S (ARS)-modified anion exchange resin or by flotation of U-ARS chelate, Separation Science and Technology, 33, **1998**, 2123-2141. https://doi.org/10.1080/01496399808545719.

[5] **A.M. Atta, Z.M. Abdel_Wahab, Z.A. El_Shafy, W.I. Zidan, Z.F. Akl,** Uranyl ions uptake from aqueous solutions using crosslinked ionic copolymer based on 2-Acrylamide-2-methylpropane sulfonic acid copolymer, Journal of Dispersion Science and Technology, 31, **2010**, 1606-1610. https://doi.org/10.1080/01932690903296977.

[6] **A.M. Atta, A.A. Abdel_Rahman, I.E. Aassy, F.Y. Ahmed, M.F. Hamza,** Adsorption Properties of Uranium (VI) Ions on Reactive CrosslinkedAcrylamidoxime and Acrylic Acid Copolymer Resins, Journal of Dispersion Science and Technology, 32(1), **2010**, 84-94. https://doi.org/10.1080/00377990903543053.

[7] **M.F. Cheira, A.M. El-Didamony, K.F. Mahmoud, B.M. Atia,**Equilibrium and kinetic characteristics of uranium recovery by the strong base Ambersep 920U Cl resin, IOSR-AC, 7, **2014**, 32-40. https://doi.org/10.9790/5736-07533240.

[8] **M.F. Cheira,**Characteristics of uranium recovery from phosphoric acid by amino phosphonic acid resin and application to wet process phosphoric acid, European Journal of Chemistry, 6(1), **2015**, 48-56. https://doi.org/10.5155/eurjchem.6.1.48-56.11.

[9] **Bahig Atia,** Synthesis, characterization, and physico-chemical aspects of a new PVC-based quaternary triethanol ammonium chloride anionite for tungsten recovery, Turkish Journal of Chemistry, 48, **2024**. https://doi.org/10.3390/kim-2310-33 .

[10] **M. Merdivan, M.Z. Duz, C. Hamamci,** Sorption behavior of uranium (VI) with N,N-dibutyl-N¯-benzoyl thiourea impregnated in Amberlite XAD-16, Talanta, 55, **2001**, 639-645.

[11] **M.S. Hosseini, A.H. Bandegharaei,** Comparison of sorption behavior of Th(IV) and U(VI) on modified impregnated resin containing quinizarin with conventional prepared impregnated resin, Hazardous Materials, 190, **2011**, 755-765. https://doi.org/10.1016/j.jhazmat.2011.03.111.

[12] **M.A. Maheswari, M.S. Subramanian,** Selective enrichment of U(VI), Th(IV) and La(III) from high acidic streams using a new chelating ion exchange polymeric matrix, Talanta, 64(1), **2004**, 202-209. https://doi.org/10.1016/j.talanta.2004.02.029.

[13] **M.A. Maheswari, M.S. Subramanian,** AXAD-16-3,4-dihydroxyl benzoyl methyl phosphonic acid: A selective preconcentration of U(VI) and Th(IV) from acidic waste streams and environmental samples, React. Funct.Polym., 62(1), **2005**, 105-114. https://doi.org/10.1016/j.reactfunctpolym.2004.10.001.

[14] **D. Prabhakaran, M.S. Subramanian,** A column system for the selective extraction of U(VI) and Th(IV) using a new chelating sorbent , Talanta, 61(4), **2003**, 423-430. https://doi.org/10.1016/S0039-9140(03)00308-4.

[15] **N. Kabay, M. Demircioglu, S. Yayh, E. Gunay, M. Yuksel, M. Saglam, M. Streat,** Recovery of uranium from phosphoric acid solutions using chelating ion exchange resins , Ind. Eng. Chem. Res., 37, **1998**, 1983-1990. https://doi.org/10.1021/ie970518k.

[16] **A.A. Atia,** Studies on the interaction of mercury II and uranyl II with modified chitosan resins, Hydrometallurgy, 80, **2005**, 13-22. https://doi.org/10.1016/j.hydromet.2005.03.009.

[17] **C.S. Raju, M.S. Subramanian,** Sequential separation of lanthanides, thorium and uranium using novel solid phase extraction method from high acidic nuclear wastes, Hazardous Materials, 145, **2007**, 315-322. https://doi.org/10.1016/j.jhazmat.2006.11.024.

[18] **C.S. Raju, M.S. Subramanian,** A novel solid phase extraction method for separation of actinides and lanthanides from high acidic streams, Separation and Purification Technology, 55(1), **2007**, 16-22. https://doi.org/10.1016/j.seppur.2006.10.013.

[19] **B.N. Singh, B. Maiti,** Separation and preconcentration of U(VI) on AXAD-4 modified with 8-hydroxy quinoline , Talanta, 69(2), **2006**, 393-396. https://doi.org/10.1016/j.talanta.2005.06.072.

[20] **R. Burgada, T. Bailly, T. Prange, M. Lecouvey,** Synthetic strategy of new powerful tris-biphosphonic ligands for chelation of uranium, iron and cobalt cations, Tetrahed.Lett., 48(13), **2007**, 2315-2319. https://doi.org/10.1016/j.tetlet.2007.01.155.

[21] **V.K. Jain, R.A. Pandy, S.G. Pillai,** Simultaneous preconcentration of uranium (VI) and thorium (IV) from aqueous solutions using a chelating calix[4]arene anchored chloromethylated polystyrene solid phase, Talanta, 70(2), **2006**, 257-266. https://doi.org/10.1016/j.talanta.2006.02.032.

[22] **F.A. Aydin, M. Soylak,** Solid phase extraction and preconcentration o on Duolite XAD-761 prior their inductively coupled plasma spectrometric determination, Talanta, 72(1), **2007**, 187-192. https://doi.org/10.1016/j.talanta.2006.10.013.

[23] **M. Nogami, I.M. Ismail, M. Yamaguchi, K. Suzuki,** Synthesis characterization and some adsorption properties of TMMA chelating resin, Sol. Stat. Chem., 171, **2003**, 353-357. https://doi.org/10.1016/S0022-4596(02)00233-5.

[24] **K. Dev, R. Pathak, G.N. Rao,** Sorption behavior of La(III), Nd(III), Th(IV) Tb(III) and U(VI) on Amberlite XAD-4 functionalized with bicine ligand, Talanta, 48, **1999**, 579-584.https://doi.org/10.1016/s0039-9140(98)00274-4.

[25] **D. Prabhakaran, M.S. Subramanian,** Selective extraction and sequential separation of actinide and transition ion using AXAD-16-BTBED polymeric sorbent, React. Funct.Polym., 57, **2003**, 147-155. https://doi.org/10.1016/j.reactfunctpolym.2003.09.003.

[26] **U.V. Trivedi, S.K. Menon, Y.K. Agrawal,** Polymer supported calix[6]arenehydroxamic acid, a novel chelating resin, React. Funct.Polym., 50, **2002**, 205-216. https://doi.org/10.1016/S1381-5148(01)00106-7.

[27] **R. Pathak, G.N. Rao,** Synthesis and metal sorption studies of p-tert-butyl calix[8]arene chemically bounded to polymeric support, Anal. Chim.Acta, 335, **1996**, 283-290. https://doi.org/10.1016/S0003-2670(96)00372-8.

[28] **C.S. Raju, M.S. Subramanian,** DAPPA grafted polymer: an efficient solid phase extractant for U(VI), Th(IV) and La(III) from acidic waste streams and environmental samples, Talanta, 67, **2005**, 81-89. https://doi.org/10.1016/j.talanta.2005.02.003.

[29] **M. Nogami, T. Nishida, N. Miyata,**Adsorptivity of novel cyclic monoamide resin for selective separation of U(VI) in nitric acid media, Energy Procedia, 39, **2013**, 96 -101,https://doi.org/10.1016/j.egypro.2013.07.195.

[30] **D.H. Philips, B. Gu, D.B. Watson, C.S. Parmele,** Uranium removal from contaminated ground water by synthetic resins, Water Research, 42, **2008**, 260-268. https://doi.org/10.1016/j.watres.2007.07.010.

[31] **T.S. Mokhtari, E. Sheikhhosseini, M.A. Amrollahi, H. Sheibani**, A convenient one-pot synthesis of novel tetraamides via 2-cyclopentylidenemalonic acid based Ugi-four component reaction, Journal of Saudi Chemical Society, 21(3), **2017**, 300-305.https://doi.org/10.1016/j.jscs.2015.07.008.

[32] **R.M. Lanigan, T.D**. Sheppard, Recent developments in amide synthesis: Direct amidation of carboxylic acids and transamidation reactions, European Journal of Organic Chemistry, 33, **2013**, 7453-7465. https://doi.org/10.1002/ejoc.201300573.

[33] **B.K. Zambron, S.R. Dubbaka, D. Markovic, E. Moreno-Clavijo, P. Vogel** , Amide Formation in One Pot from Carboxylic Acids and Amines via Carboxyl and Sulfinyl Mixed Anhydrides, Organic letters, 15(10), **2013**, 2550-2553.https://doi.org/10.1021/ol401053y.

[34] **Z. Marczenko, M. Balcerzak,** Separation, preconcentration and spectrophotometry in inorganic analysis, Elsevier Science B.V., Amesterdam, Netherland, **2000**, 446-455.

[35] **W. Davies, W. Gray,** A rapid and specific volumetric method for the precise determination of uranium using ferrous sulfate as a reductant, Talanta, 11(8), **1964**, 1203-1211. https://doi.org/10.1016/0039-9140(64)80171-5.

[36] **K.J. Mathew, B. Mason, M.E. Morales, U.I. Narayann,** Uranium assay determination using Davies and Gray titration: An overview and implementation of GUM uncertainty evaluation, Radioanalytical and Nuclear Chemistry, 282, **2009**, 939-944.https://doi.org/10.1007/s10967-009-0186-4.

[37]**B.M. Atia, A.K. Sakr, M.A. Gado, H.S. El-Gendy, N.M. Abdelazeem, E.M. El-Sheikh, M.Y. Hanfi, M.I. Sayyed, J.S. Al-Otaibi, M.F. Cheira,** Synthesis of a New Chelating Iminophosphorane Derivative (Phosphazene) for U(VI) Recovery, Polymers**, 2022**, 14, 1687. https://doi.org/10.3390/polym14091687.

[38] **P. Jia, L. Hu, Q. Shang, R. Wang, M. Zhang, Y. Zhou,** Self-Plasticization of PVC Materials via Chemical Modification of Mannich Base of Cardanol Butyl Ether, ACS Sustainable Chem. Eng., 5, **2017**, 6665-6673. https://doi.org/10.1021/acssuschemeng.7b00900.

[39] **N.S. Alghunaim,** Spectroscopic analysis of PMMA/PVC blends containing $CoCl_2$, Results in Physics, 5 **2015**, 331–336. http://dx.doi.org/10.1016/j.rinp.2015.11.003.

[40] **E. Rusen, R. S.¸omoghi, C. Busuioc, A. Diacon,** Hydrophilic modification of polyvinyl chloride with polyacrylic acid using ATRP, RSC Adv., **2020**, 10, 35692. http://dx.doi.org/10.1039/d0ra05936f.

[41] **M.F. Cheira , B.M. Atia, M.N. Kouraim,** Uranium(VI) recovery from acidic leach liquor by Ambersep 920U SO_4 resin: Kinetic, equilibrium and thermodynamic studies, Journal of Radiation Research and Applied Sciences, 10, **2017**, 307-319. https://doi.org/10.1016/j.jrras.2017.07.005.

[42] **Y. Suzuki, T. Nankawa, T. Yoshida, T. Ozaki, T. Ohnuki, A.J. Francis, S. Tsushima, Y. Enokida, I. Yamamoto**, Reduction behavior of uranium in the presence of citric acid, Radiochim. Acta, 94, **2006,** 579–583. https://doi.org/10.1524/ract.2006.94.9.579.

[43]**R.Vafazadeh, G.Zare-Sadrabadi**, Kinetics and Mechanism of the Ligand Exchange ReactionBetween TetraazaMacrocycle Ligand and Cu(II)Tetradentate Amine-Amide Complexes, ActaChim. Slov.,**2015**, 62, 889–894. https://doi.org/10.17344/acsi.2015.1611.

[44] **H.A. Ibrahium, M.M. Abdel Aal, N.S. Awwad, B.M. Atia, H.E. Ali, M.A. Gado, R.A. Hakami, M.F. Cheira,** Solid–liquid separation of V(V) from aqueous medium by 3-(2-hydroxy phenyl)-imino-1-phenyl butan-1-one Schiff base immobilized XAD-2 resin, International Journal of Environmental Science and Technology, **2022**, https://doi.org/10.1007/s13762-022-04465-5.

[45] **A.R. Weshahy, A.K. Sakr, A.A. Gouda, B.M. Atia, H.H. Somaily, M.Y. Hanfi, M.I. Sayyed, R. El Sheikh, E.M. El-Sheikh, H.A. Radwan, M.F. Cheira, M.A. Gado,** Selective Recovery of Cadmium, Cobalt, and Nickel from Spent Ni–Cd Batteries Using Adogen® 464 and Mesoporous Silica Derivatives, International Journal of Molecular Sciences, 23, **2022**, 8677, https://doi.org/10.3390/ijms23158677.

[46] **A.R. Weshahy, A.A. Gouda, B.M. Atia, A.K. Sakr, J.S. Al-Otaibi, A. Almuqrin, M.Y. Hanfi, M.I. Sayyed, R. El Sheikh, H.A. Radwan, F.S. Hassen, M.A. Gado,** Efficient Recovery of Rare Earth Elements and Zinc from Spent Ni–Metal Hydride Batteries: Statistical Studies, Nanomaterials**,** 12, **2022**, 2305. https://doi.org/10.3390/nano12132305.

[47] **A. Alharbi, A.A. Gouda, B.M. Atia, M.A. Gado, A.A. Alluhaybi, J. Alkabli,** The Role of Modified Chelating Graphene Oxide for Vanadium Separation from Its Bearing Samples, Russian Journal of Inorganic Chemistry, **2022**. https://doi.org/10.1134/S0036023622040027.

[48] **L. Irving.,** The adsorption of gases on plane surfaces of glass, mica and platinum, American Chemical Society, 40, **1918**, 1361-1368. https://doi.org/10.1021/ja02242a004.

[49] **B.M. Atia, Y.M. Khawassek, G.M. Hussein, M.A. Gado, M.A. El-Sheify, M.F. Cheira,** One-pot synthesis of pyridine dicarboxamide derivative and its application for uranium separation from acidic medium, Journal of Environmental Chemical Engineering, 9, **2021**, 105726. https://doi.org/10.1016/j.jece.2021.105726.

[50] **B.M. Atia, M.A. Gado, M.O. Abd El-Magied, E.A. Elshehy,** Highly efficient extraction of uranyl ions from aqueous solutions using multi-chelators functionalized graphene oxide, Separation Science and Technology, **2019**. https://doi.org/10.1080/01496395.2019.1650769.

[51] **M.A. Gado, B.M. Atia, M.F. Cheira, M.E. Elawady, M. Demerdash,** Highly efficient adsorption of uranyl ions using hydroxamic acid-functionalized graphene oxide, Radiochim. Acta, **2021**.https://doi.org/10.1515/ract-2021-1063.

[52] **H.A. Ibrahium, N.S. Awwad, Mohamed A. Gado, Mohamed A. Hassanin, A.A. Nayl, Bahig M. Atia,** Physico-Chemical Aspects on Uranium and Molybdenum Extraction from Aqueous Solution by Synthesized Phosphinimine Derivative Chelating Agent, Journal of Inorganic and Organometallic Polymers and Materials, **2022**. https://doi.org/10.1007/s10904-022-02374-1.

[53] **S.R. Al-Mhyawi, D.M.D. Bader, M.A. Bajaber, S.M. Abd El Dayem, A.H. Ragab, K. . Abd El-Rahem, M.A. Gado, B.M. Atia, M.F. Cheira,** Zirconium oxide with graphene oxide anchoring for improved heavy metal ions adsorption: Isotherm and kinetic study, Journal of Materials Research and Technology, 22, **2023**, 3058-3074. https://doi.org/10.1016/j.jmrt.2022.11.121.

[54] **X. Yang, M. Cui, R. Su, R. Huang,**The Preparation of a Polyamidoxime–Phosphorylated Cellulose Nanofibrils Composite Aerogel for the Selective Extraction of Uranium from Seawater, Nanomaterials, 14, **2024**, 1297. https://doi.org/10.3390/nano14151297.

[55] **D. Emre, O.S. Zorer, A. Bilici, E. Budak, S. Yilmaz, N.C. Kilic, E.G. Sogut,** Adsorption of uranium (VI) from aqueous solutions using boron nitride/polyindole composite adsorbent, Journal of Applied Polymer Science, 141, **2024**, e54856. https://doi.org/10.1002/app.54856.

[56] **G. Shelar-Lohar, S. Joshi,** Comparative study of uranium and thorium metal ion adsorption by gum ghatti grafted poly(acrylamide) copolymer composites, RSC Adv., 9, **2019**, 41326. https://doi.org/10.1039/c9ra08212c.

[57] **C. Lv, L.P. Liu, J.H. He, L. Yang, J.T. Liu, C.Q. Xia, X.Y. Huang, M.L. Fing,** Efficient uranium adsorption of low-cost and eco-friendly MQ_2-collagen fibers (M = Mo, W; Q = S, Se) composite materials prepared by co-ball milling, National Science Open, 4, **2025**, 20240029. https://doi.org/10.1360/nso/20240029.

[58] **Z.F. Akl, E.G. Zaki, S.M. El-Saeed,** Green Hydrogel-Biochar Composite for Enhanced Adsorption of Uranium, ACS Omega, 6, **2021**, 34193−34205. https://doi.org/10.1021/acsomega.1c01559.

[59] **M.F. Hamza, H.A. Abu Khoziem, M.S. Khalafalla, W.M. Abdellah, D.I. Zaki, K. Althumayri, Y. Wei,** Ecofriendly Composite as a Promising Material for Highly-Performance Uranium Recovery from Different Solutions, Toxics, 10, **2022**, 490. https://doi.org/10.3390/toxics10090490.

[60] **A. Gopalakrishnan, S. Asare, F. Adu-Boahene, A.I. Schafer,** Uranium adsorption by iron modifed zeolite and zeolite composite membranes, Chemosphere, 368 , **2024**, 143711. https://doi.org/10.1016/j.chemosphere.2024.143711.

[61] **M.S. Hagag, S.M. Esmaeel, F. Salem, A.H. Ali, S.A. Zaki,** Thermal activation of kaolinite titanium hydroxide composite for uranium adsorption from aqueous solutions, International Journal of Environmental Science and Technology, 20, **2023**, 9041–9052. https://doi.org/10.1007/s13762-022-04533-w.